SAND2019-0644C

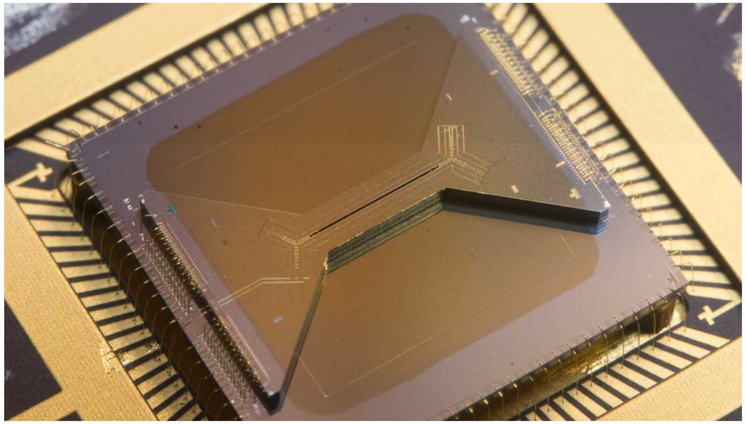

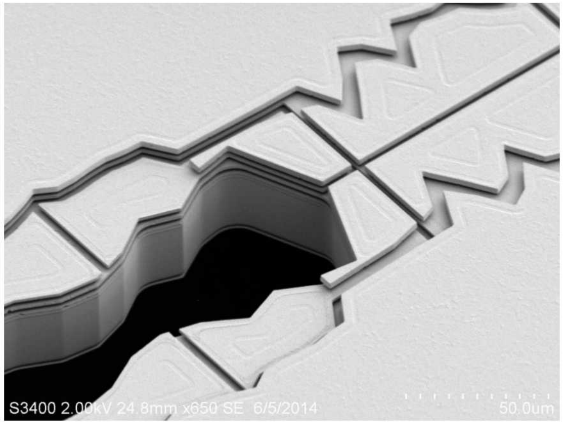

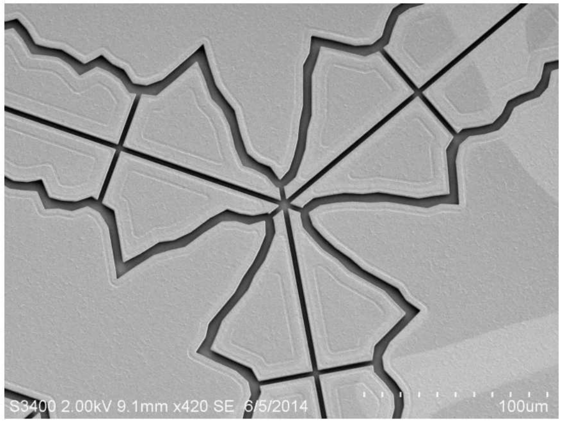

High-fidelity quantum and classical control in microfabricated surface ion traps

Daniel Lobser

Sandia National Laboratories

I A R P A

LABORATORY DIRECTED RESEARCH & DEVELOPMENT

U.S. DEPARTMENT OF ENERGY

NNSA National Nuclear Security Administration

Sandia National Laboratories is a multimission laboratory managed and operated by National Technology & Engineering Solutions of Sandia, LLC, a wholly owned subsidiary of Honeywell International, Inc., for the U.S. Department of Energy's National Nuclear Security Administration under contract DE-NA0003525.

Motivation

Quantum Information

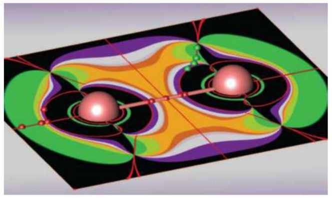

Quantum chemistry

- Calculation of molecular potentials
- Nitrogen and Oxygen fixation, development of catalytic converters

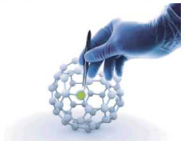

Medicine

- Structure-based drug development

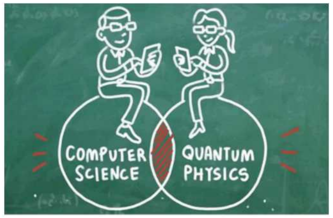

Quantum computing

- Number factorization (Shor's algorithm)
- Search in unstructured data, searching for solutions to hard problems (Grover's search algorithm)

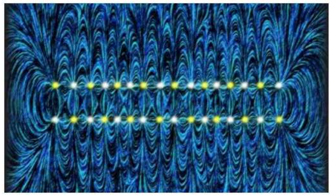

Quantum simulation

- Simulating many-body systems
- Already for about 20 qubits not possible to simulate classically.

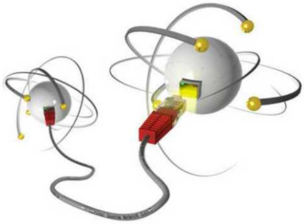

Quantum Communication

- Securing a quantum channel

Qubit Implementations

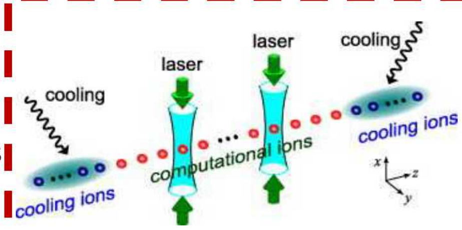

Trapped Ions

- Blatt and Wineland "Entangled States of Trapped Atomic Ions." *Nature* 453, 1008–15 (2008).
- Monroe and Kim. "Scaling the Ion Trap Quantum Processor." *Science* 339, 1169 (2013)

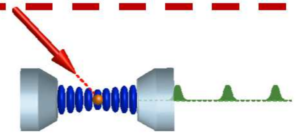

Neutral Atoms

- Rydberg states
- Atoms in cavities

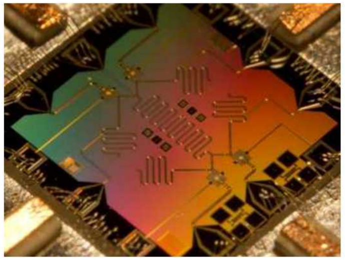

Superconducting Josephson junctions

- Devoret and Schoelkopf. "Superconducting Circuits for Quantum Information: An Outlook." *Science* 339, 1169 (2013).

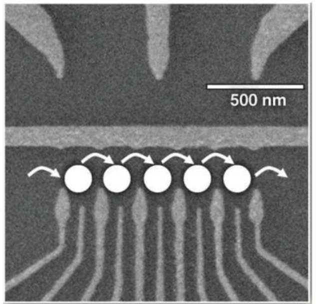

Quantum dots

- Awschalom, et al., "Quantum Spintronics: Engineering and Manipulating Atom-Like Spins in Semiconductors." *Science* 339, 1174 (2013).

Brief Overview of Ion Trapping

Earnshaw's Theorem: *Static electric fields can't create a stable confining potential for charged particles*

r.f. Paul Trap

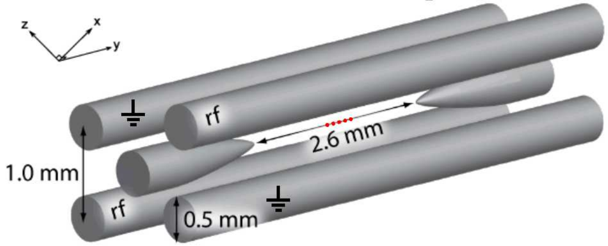

r.f. pseudopotential

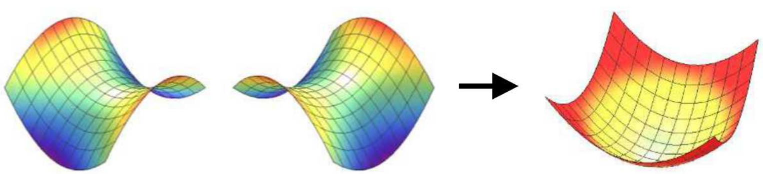

- Time-averaged potential is close to harmonic at the saddle point
- Off the saddle point, ions experience micromotion
- Works well for linear chains of ions
- Doesn't support fine control of ion position or confining potential

Segmented Paul Trap

- Better control over confining potential
- Difficult to construct
- Doesn't scale well

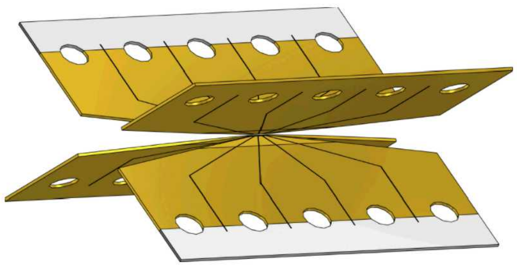

Microfabricated Surface Trap

- Consistent, well-defined electrode layout
- Microfabrication supports a lot of exotic electrode geometries
- Excellent control over potential
- Very scalable

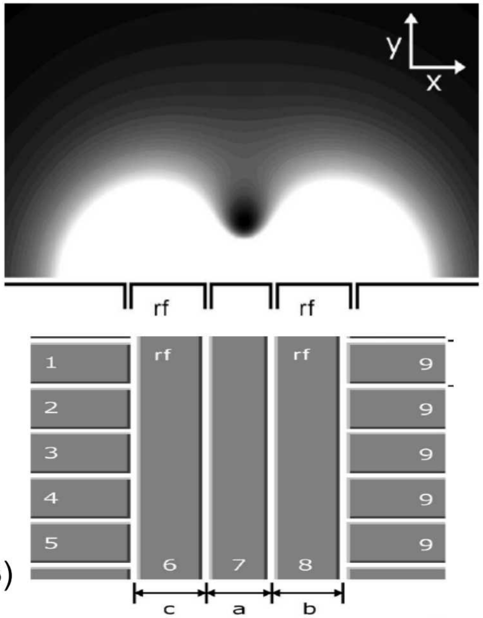

House, PRA **78** 033402 (2008)

Surface Ion Traps

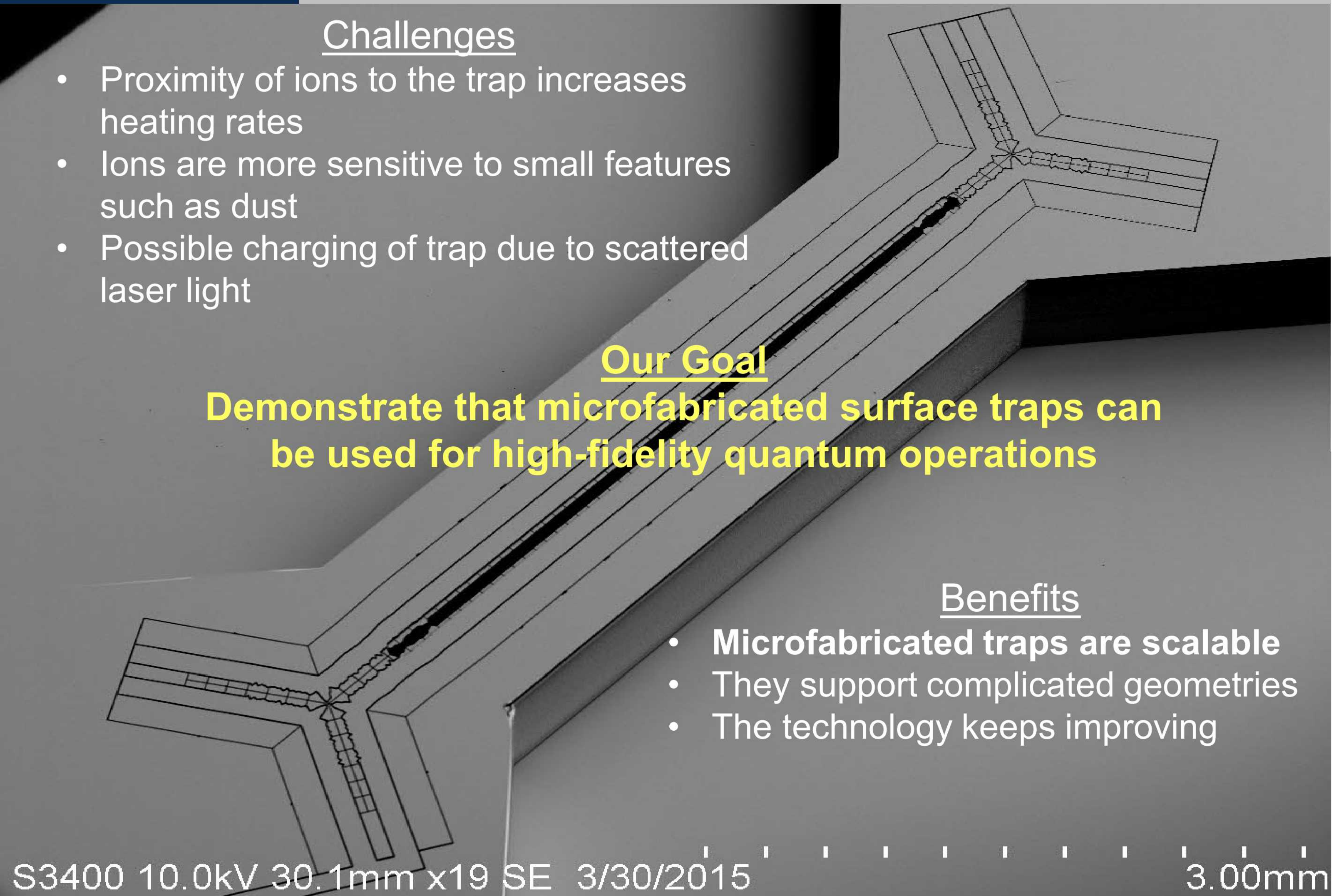

Challenges

- Proximity of ions to the trap increases heating rates
- Ions are more sensitive to small features such as dust
- Possible charging of trap due to scattered laser light

Our Goal

Demonstrate that microfabricated surface traps can be used for high-fidelity quantum operations

Benefits

- **Microfabricated traps are scalable**
- They support complicated geometries
- The technology keeps improving

Outline

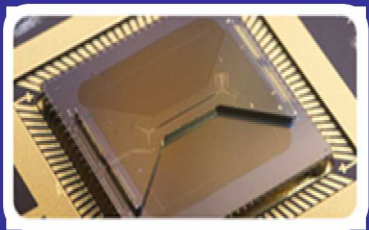

Sandia's Surface Ion Traps

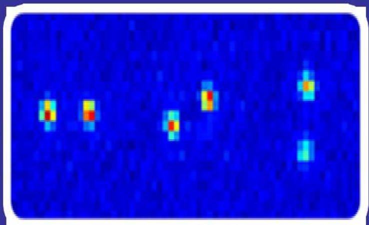

Classical Control

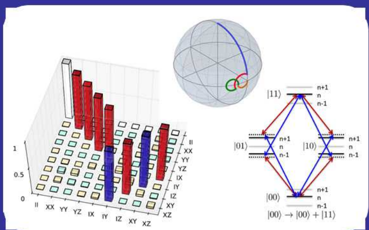

Quantum Control

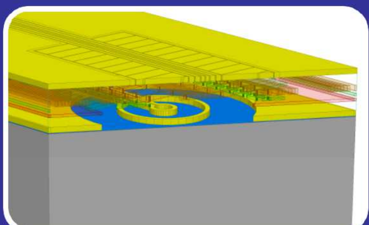

Specialized Ion Traps

Some of Sandia’s Traps

High Optical Access (HOA) trap

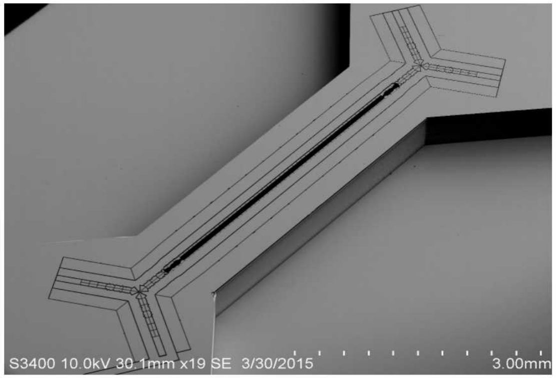

Circulator trap

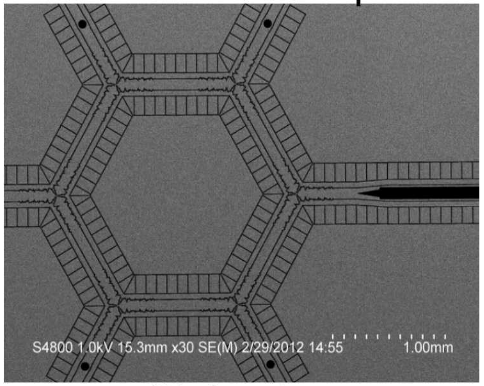

Microwave trap

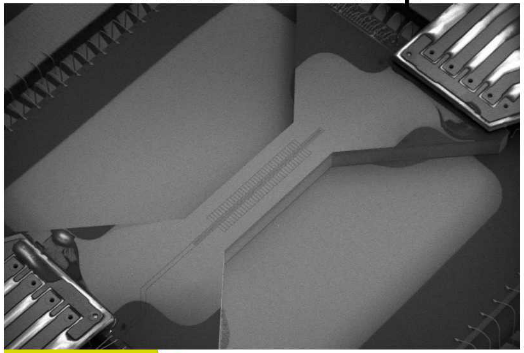

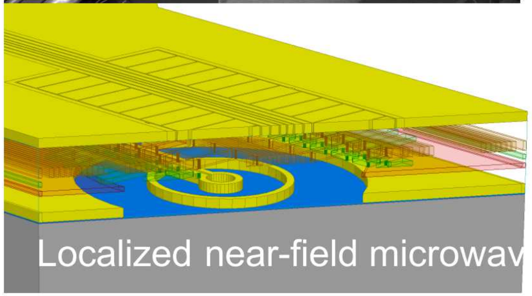

Y-junction traps

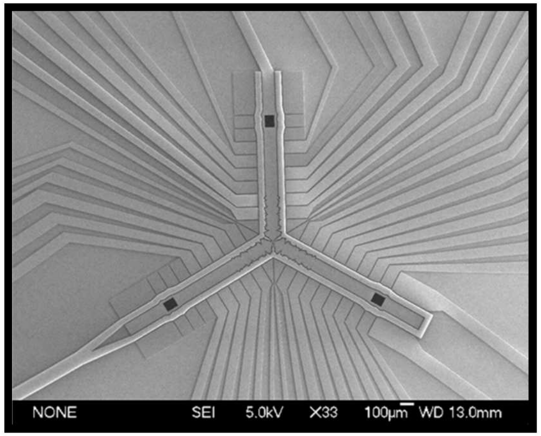

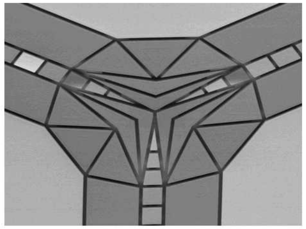

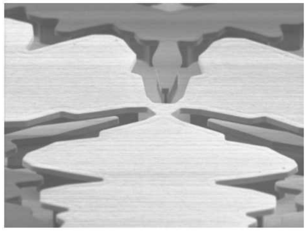

Stylus trap

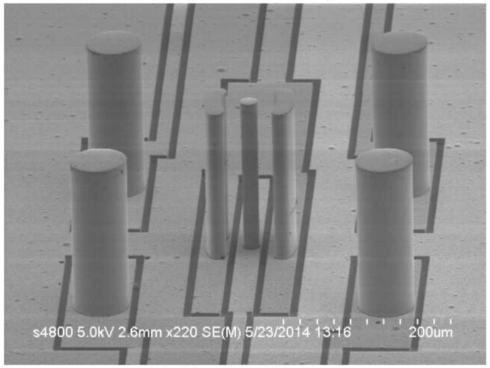

Ring trap

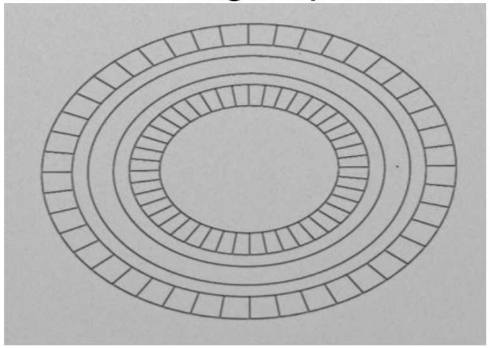

EPICS trap

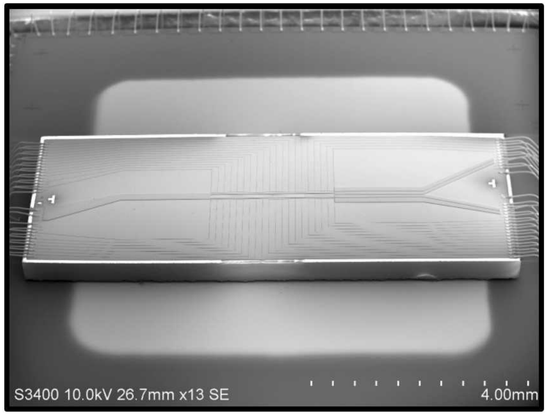

High Optical Access (HOA)

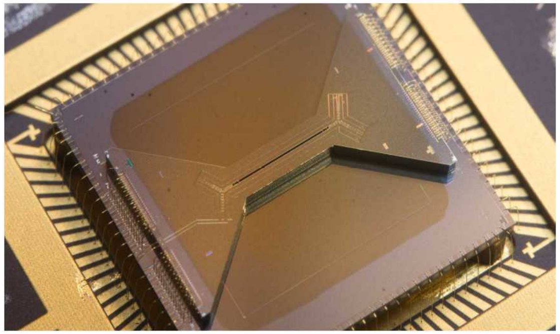

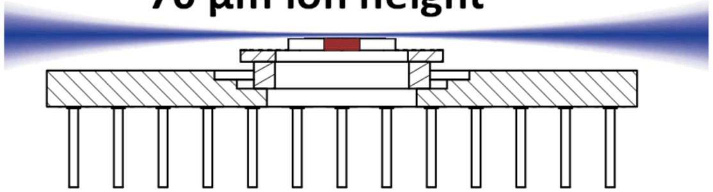

Optical access

- Excellent optical access rivaling 3D
  NA 0.25 vertical, NA 0.12 lateral

Trap strength (Typical Yb^+)

- Radial trap frequency 2 - 5 MHz
- RF frequency 50 MHz
- Stable for long ion chains
- Low heating rates (30 q/s parallel to surface, 125 q/s perpendicular)
- >100 h observed (while running measurements)
- >5 min without cooling

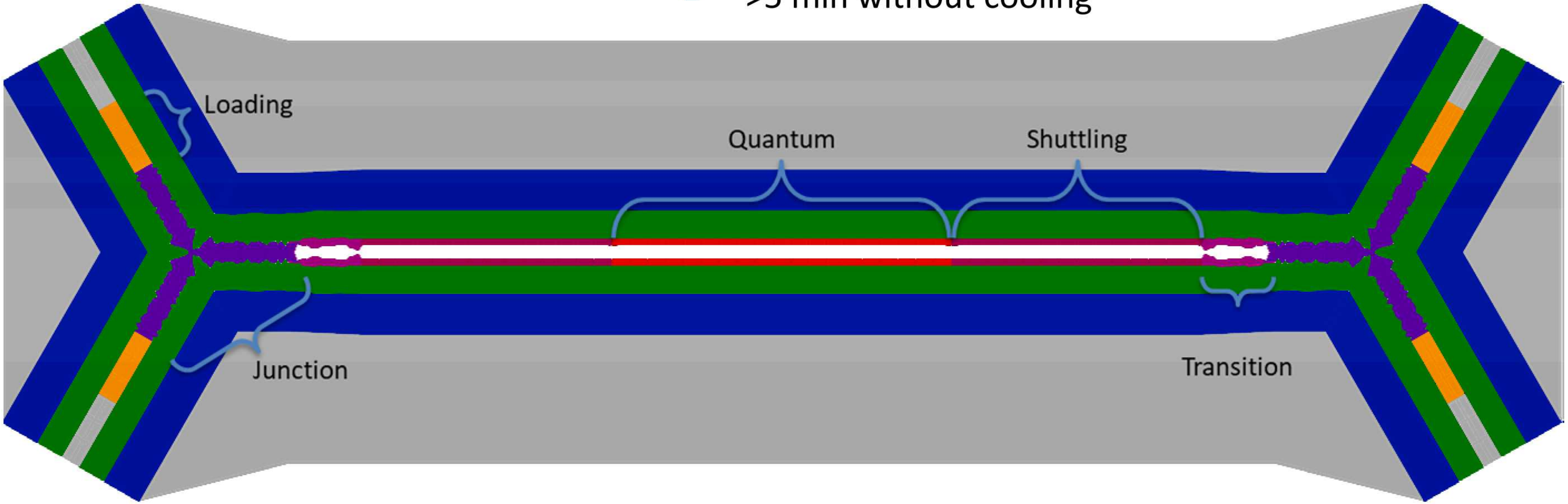

Outline

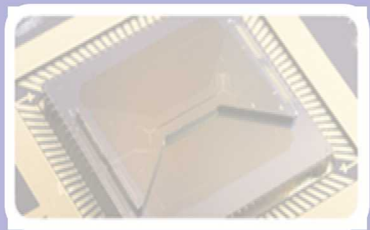

Sandia's High-Optical-Access Trap

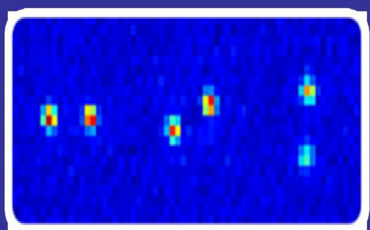

Classical Control

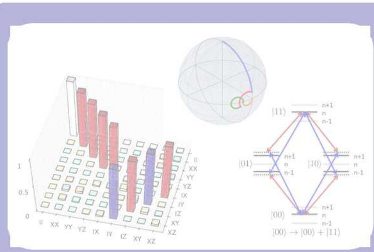

Quantum Control

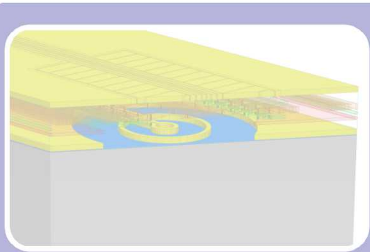

Specialized Ion Traps

Control of Confining Potential

$$\mathcal{H} = \begin{pmatrix} \frac{\partial\phi}{\partial x\partial x} & \frac{\partial\phi}{\partial x\partial y} & \frac{\partial\phi}{\partial x\partial z} \\ \frac{\partial\phi}{\partial y\partial x} & \frac{\partial\phi}{\partial y\partial y} & \frac{\partial\phi}{\partial y\partial z} \\ \frac{\partial\phi}{\partial z\partial x} & \frac{\partial\phi}{\partial z\partial y} & \frac{\partial\phi}{\partial z\partial z} \end{pmatrix}$$

- Symmetric curvature tensor
- 6 degrees of freedom
- Determines trap frequencies and principal axes rotations
- Traceless for static fields
- Trace is generated by rf pseudopotential

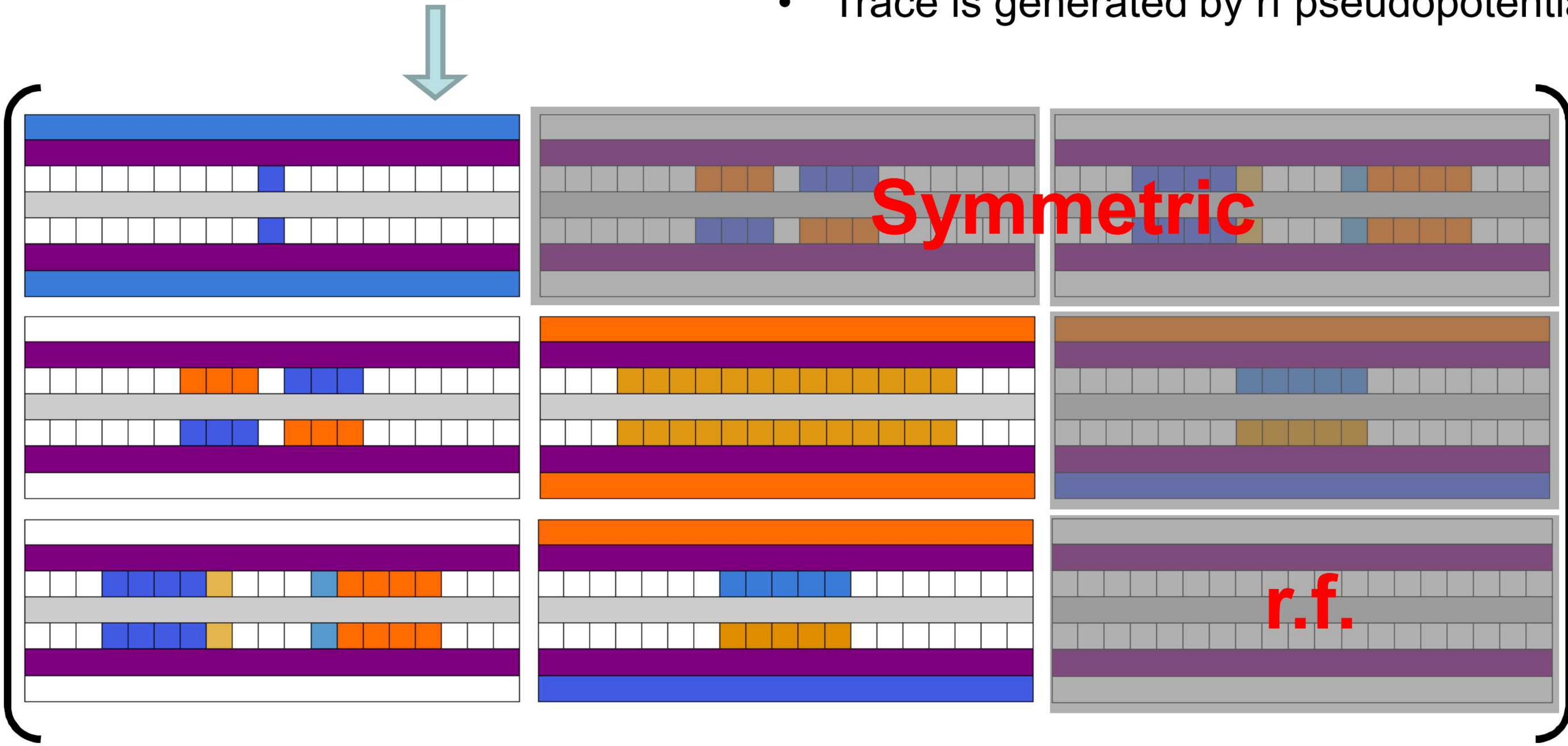

Parametric Rotation Amplitudes

$e_x,\ e_y,\ e_z$: Eigenvalues

$\partial_{xx}\phi$

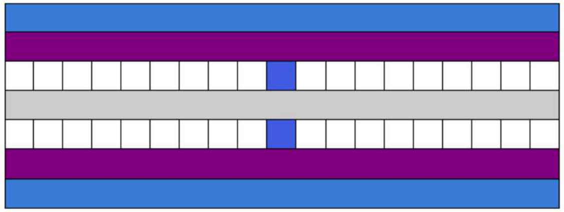

$$e_y \sin^2(\alpha) + e_x \cos^2(\alpha)$$

$\partial_{xy}\phi$

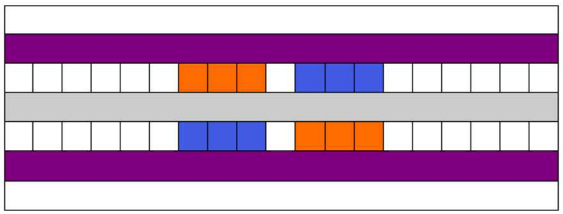

$$(e_y - e_x)\sin(\alpha)\cos(\alpha)\cos(\beta)$$

$\partial_{xz}\phi$

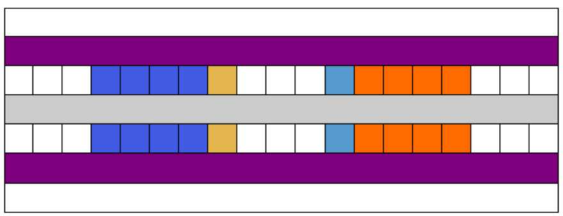

$$(e_x - e_y)\sin(\alpha)\cos(\alpha)\sin(\beta)$$

$\partial_{yy}\phi$

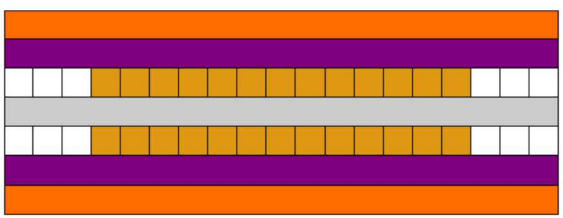

$$\left(\cos^2(\beta) - \sin^2(\beta)\right)\left(e_x \sin^2(\alpha) + e_y \cos^2(\alpha)\right) + e_z \sin^2(\beta) - e_z \cos^2(\beta)$$

$\partial_{yz}\phi$

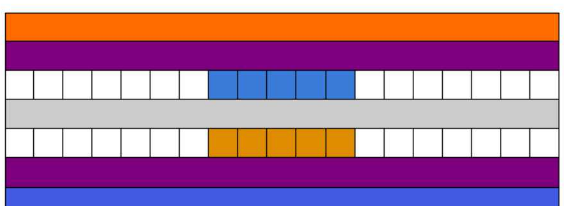

$$\sin(\beta)\cos(\beta)\left(-e_x \sin^2(\alpha) - e_y \cos^2(\alpha) + e_z\right)$$

Application To Complicated Electrode Geometries

- YZ basis (rotation of the radial axes) near the junction on the HOA 2.1
- XY basis (rotation in the plane of the trap) on the microwave trap with tied electrodes

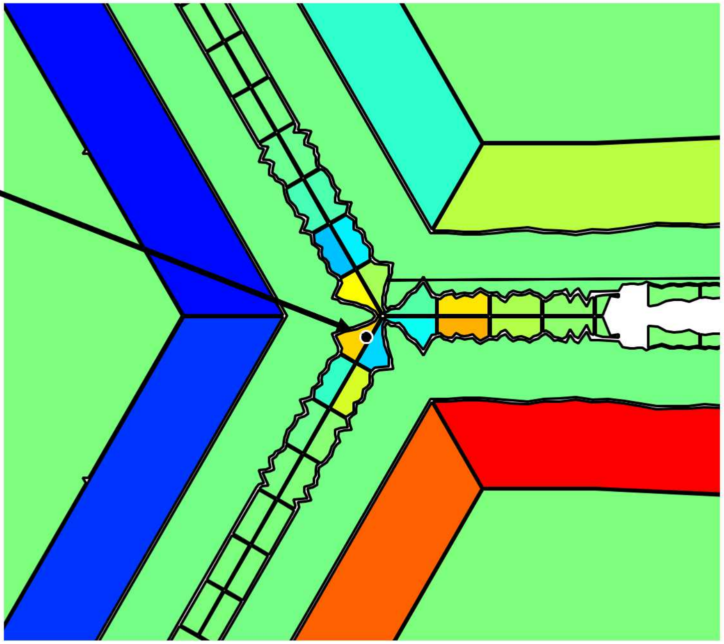

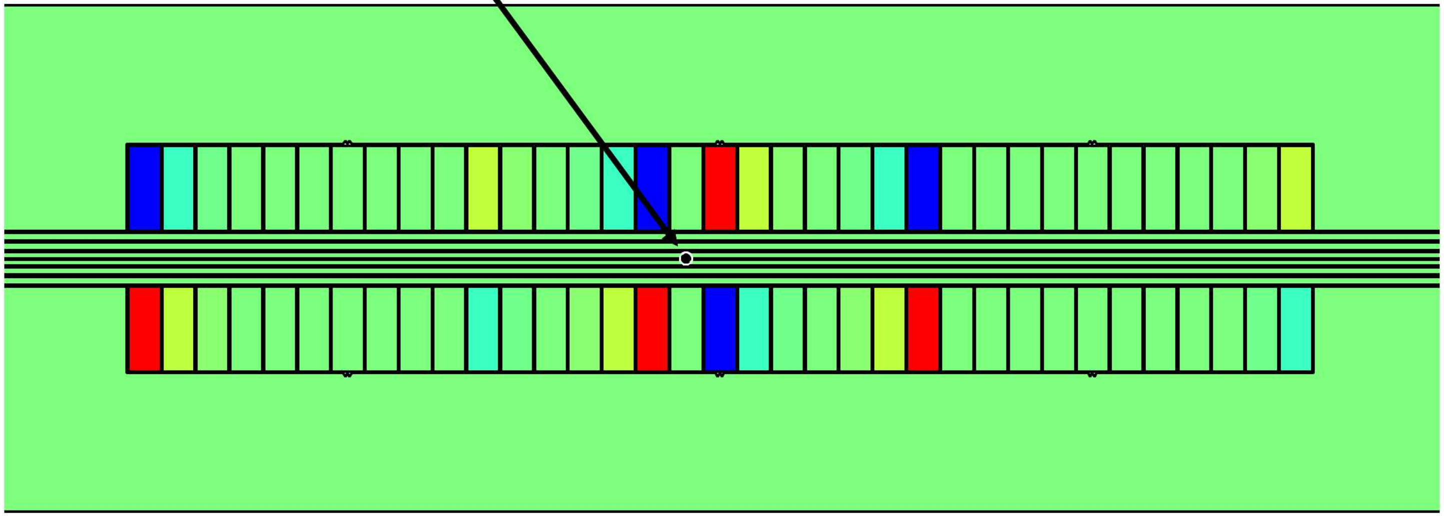

Principal Axis Rotation

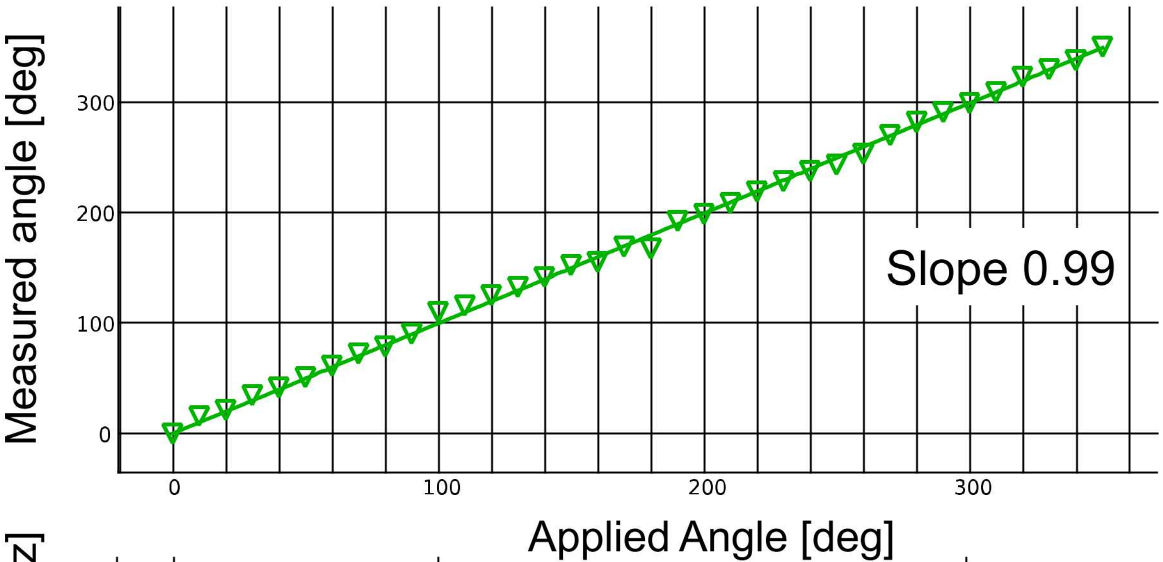

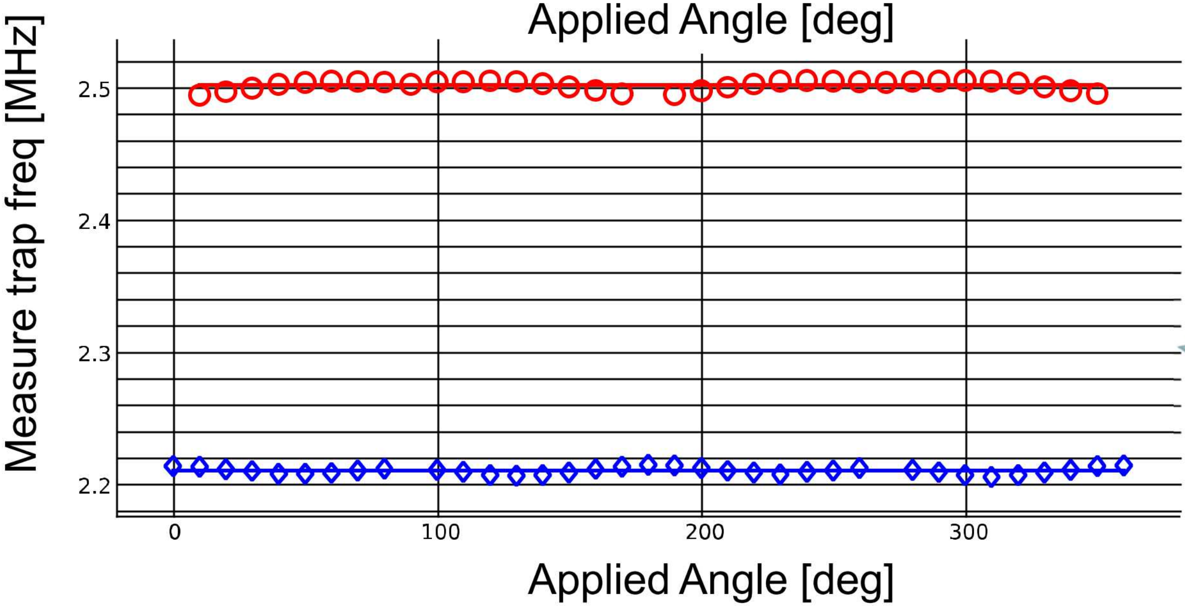

- Do we understand the trapping fields?
- Principal axes rotation realized as in simulation
- No change in trap frequencies

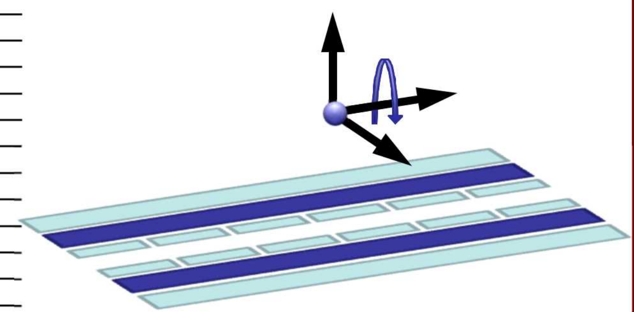

The simulations accurately describe the fields and curvatures generated by the trap

Applications

Controlled rotation

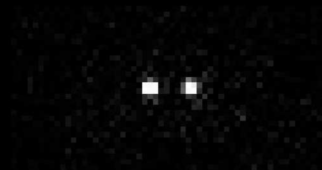

Combined rotation and translation

Separation and merging

Long Chains

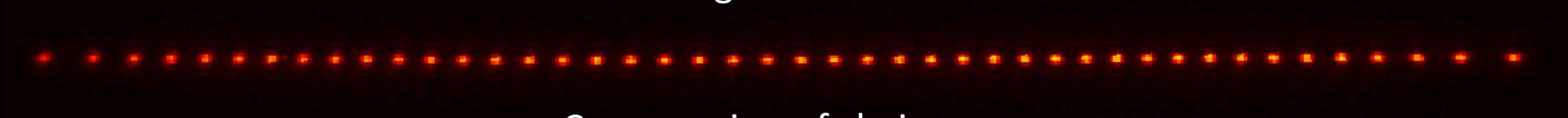

Compression of chains

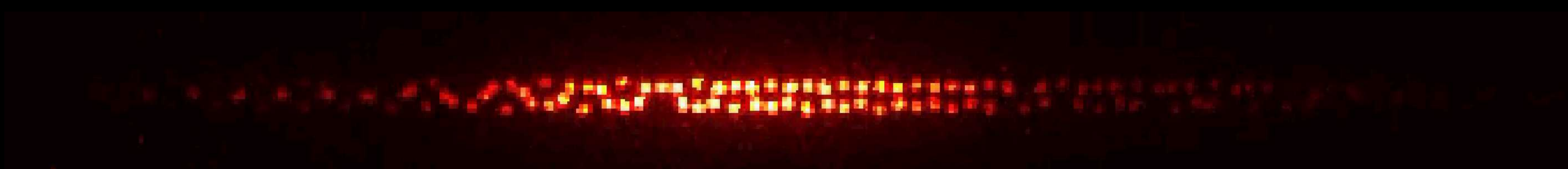

3D Crystal Structures

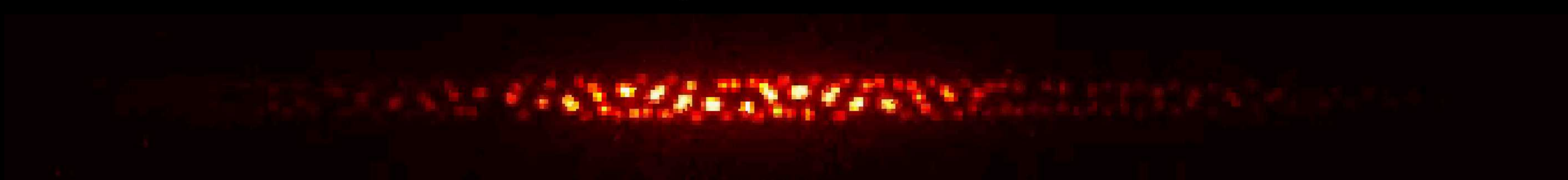

Outline

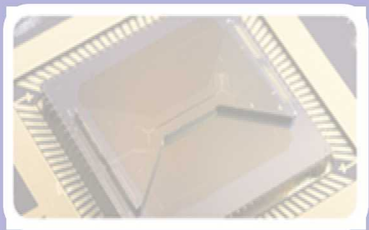

Sandia's High-Optical-Access Trap

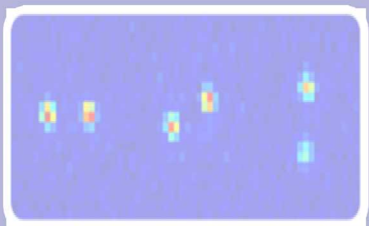

Classical Control

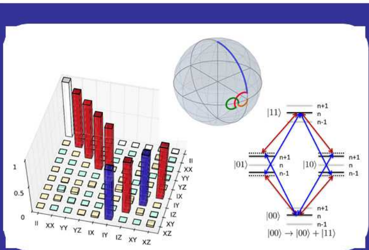

Quantum Control

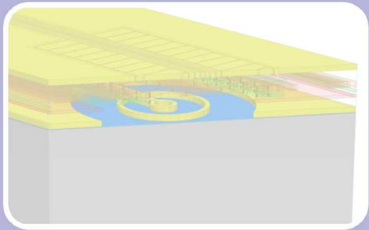

Specialized Ion Traps

The $^{171}Yb^+$ Qubit

Good clock-state qubit

Coherence time (T_2^*) > 3 s

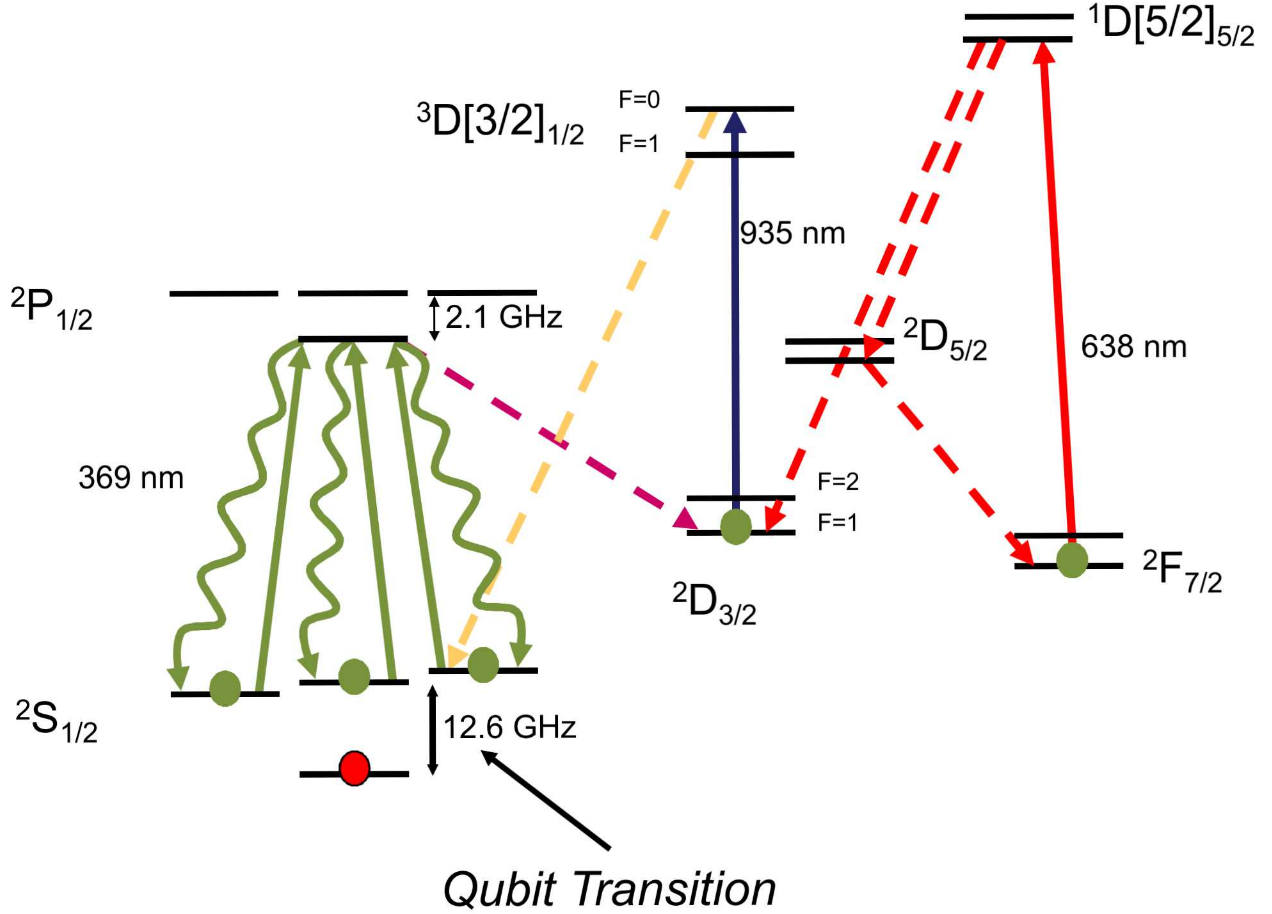

The $^{171}Yb^{+}$ Qubit

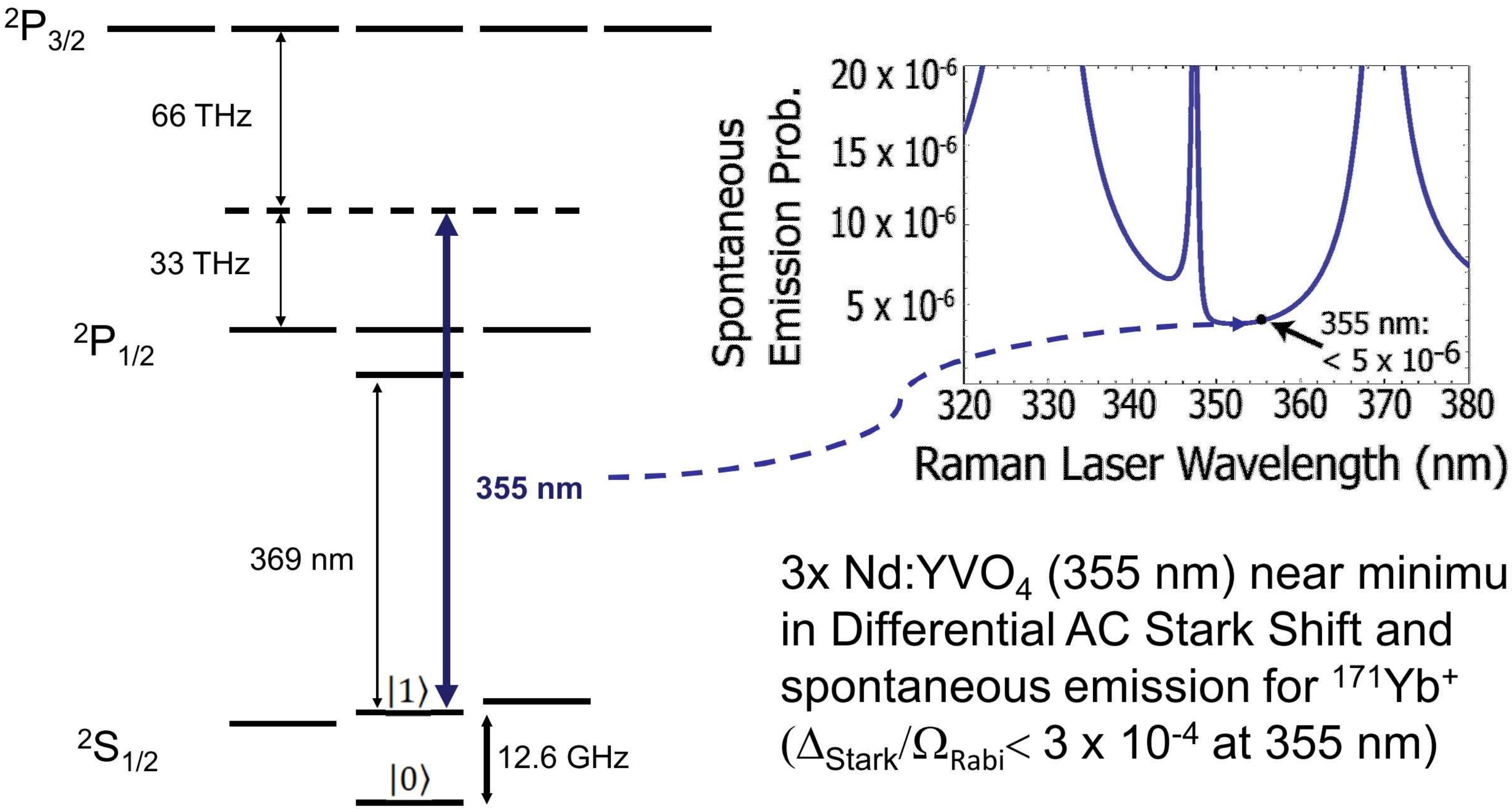

3x Nd:YVO_4 (355 nm) near minimum in Differential AC Stark Shift and spontaneous emission for $^{171}Yb^{+}$ ($\Delta_{Stark}/\Omega_{Rabi} < 3 \times 10^{-4}$ at 355 nm)

Single-Qubit Gates

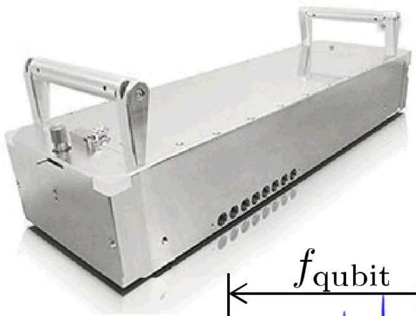

- Ions addressed via Raman transitions using a 355 nm frequency comb
- Coherent Paladin pulsed laser
  - Internal cavity is not stabilized!
  - Cavity drift leads to comb “breathing” → Corrected with repetition rate lock

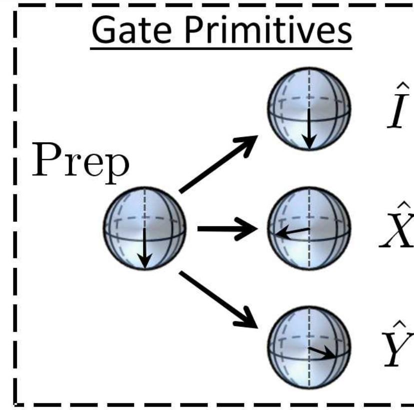

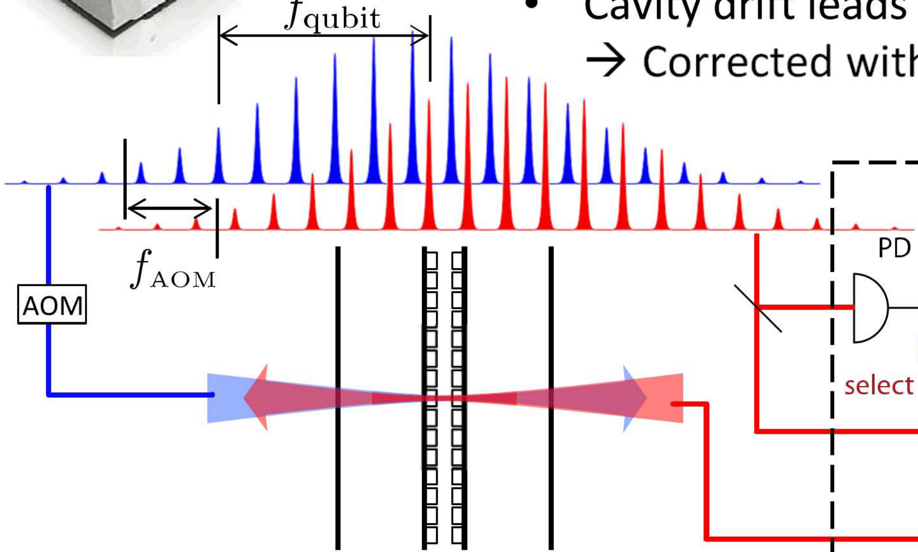

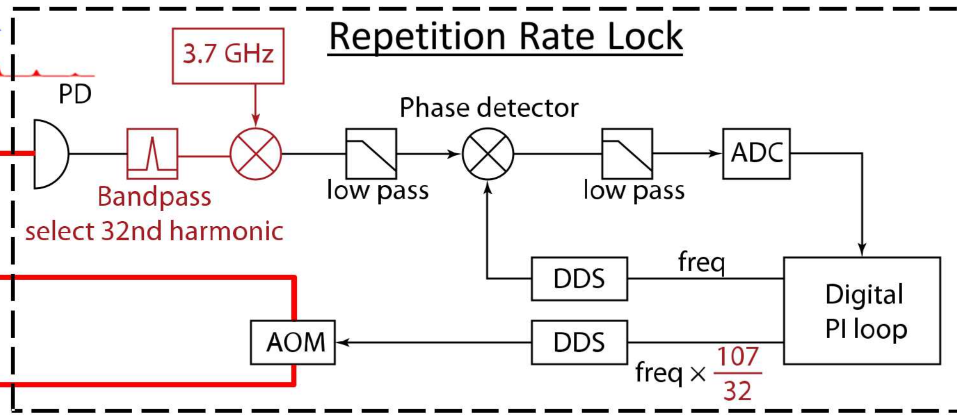

Beam Configurations

Co-propagating
- Immune to Doppler shifts
- Not affected by timing errors and pulse overlap
- Phase insensitive

Counter-propagating
- Higher overall beam intensity at ion decreases gate times
- Need for motional addressing
- Phase sensitive

Motional Addressing

Necessary for sideband cooling to motional ground states, thermometry, two-qubit gates

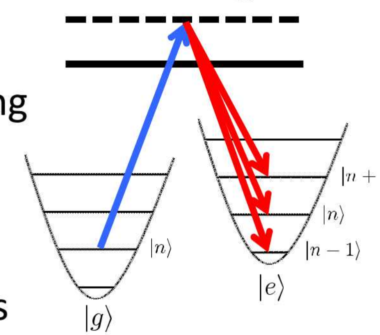

Gate Set Tomography

Developed at Sandia
www.pygsti.info

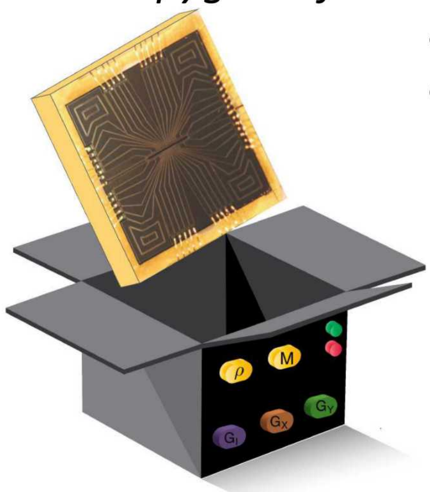

- No calibration required
- Detailed debug information
- Detects non-Markovian noise
- Uses structured sequences to amplify all possible errors
- Efficiently measures performance characterizing fault-tolerance (diamond norm)

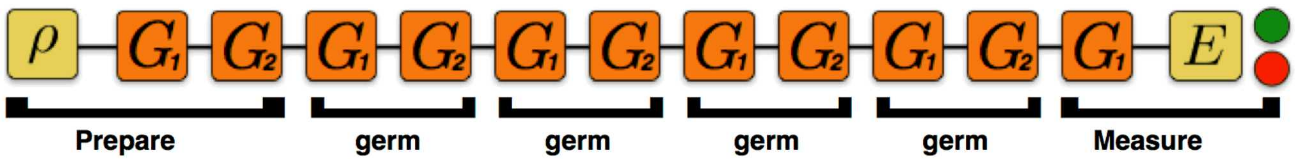

***Fiducials**: Used for preparing and measuring on all 6 poles of the Bloch sphere*
***Germs**: Carefully chosen set of gate sequences applied repeatedly*

Desired "target" gates:

G_i	Idle (Identity)
G_x	$\pi/2$ rotation about x-axis
G_y	$\pi/2$ rotation about y-axis

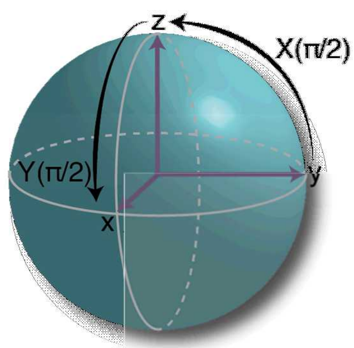

<u>Fiducials</u>

$\{\}$
Gx
Gy
$Gx \cdot Gx$
$Gx \cdot Gx \cdot Gx$
$Gy \cdot Gy \cdot Gy$

<u>Germs</u>

Gx
Gy
Gi
$Gx \cdot Gy$
$Gx \cdot Gy \cdot Gi$
$Gx \cdot Gi \cdot Gy$
$Gx \cdot Gi \cdot Gi$
$Gy \cdot Gi \cdot Gi$
$Gx \cdot Gx \cdot Gi \cdot Gy$
$Gx \cdot Gy \cdot Gy \cdot Gi$
$Gx \cdot Gx \cdot Gy \cdot Gx \cdot Gy \cdot Gy$

GST: debugging microwave gates

Gate	Rotn. axis	Angle
G_I	0.5252 −0.009 0.8506 −0.0244	0.001699π
G_X	-3×10^{-6} −1 -3×10^{-5} −0.009	0.501308π
G_Y	−0.2474 0.0001 0.9689 −0.0001	0.501366π

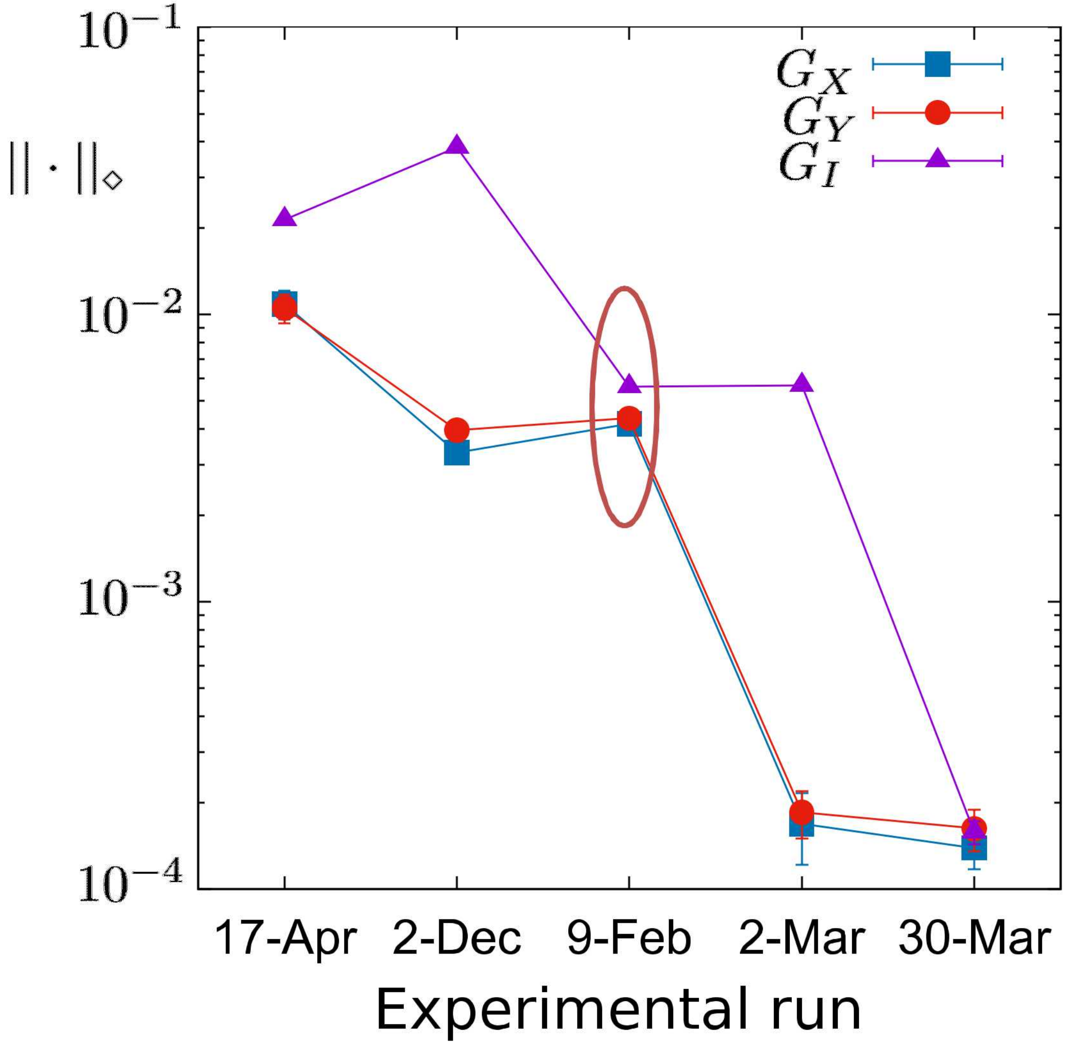

Error Mitigation

Compensated Pulses

- BB1-type dynamical-decoupling pulses used
- Corrects pulse-length errors

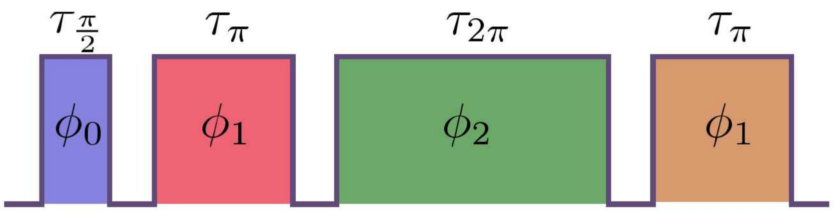

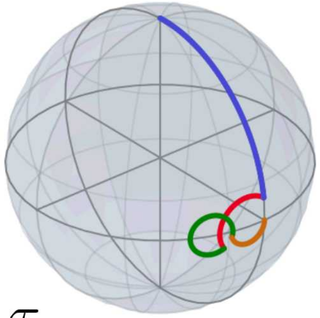

"Gapless" Pulses

- Phase changed discontinuously on DDS
- Avoids finite turn-on time effects
- Removes errors caused by asynchronous pulse arrival
- Allows for continuous power stabilization

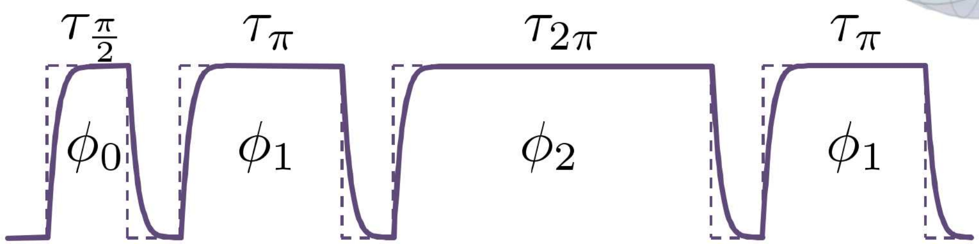

Finite turn-on time

Gapless pulse sequence

Drift Control

(Drive Frequency)

- Single-shot calibrations increase or decrease a control parameter by a negligible value
- Small corrections either average out or slowly accumulate

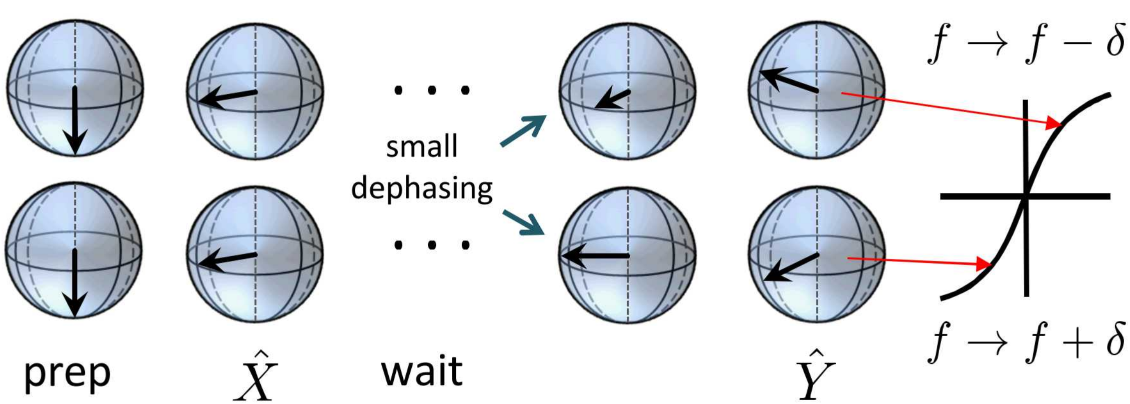

GST: debugging microwave gates

Gate	Rotn. axis	Angle
G_I	0.5252 −0.009 0.8506 −0.0244	0.001699π
G_X	-3×10^{-6} −1 -3×10^{-5} −0.009	0.501308π
G_Y	−0.2474 0.0001 0.9689 −0.0001	0.501366π

Gate	Rotn. axis	Angle
G_I	−0.0035 0.014 −0.9999 0.0006	0.001769π
G_X	-3×10^{-5} −1 1×10^{-4} 0.0006	0.500007π
G_Y	0.1104 4×10^{-5} 0.9939 0.0005	0.50001π

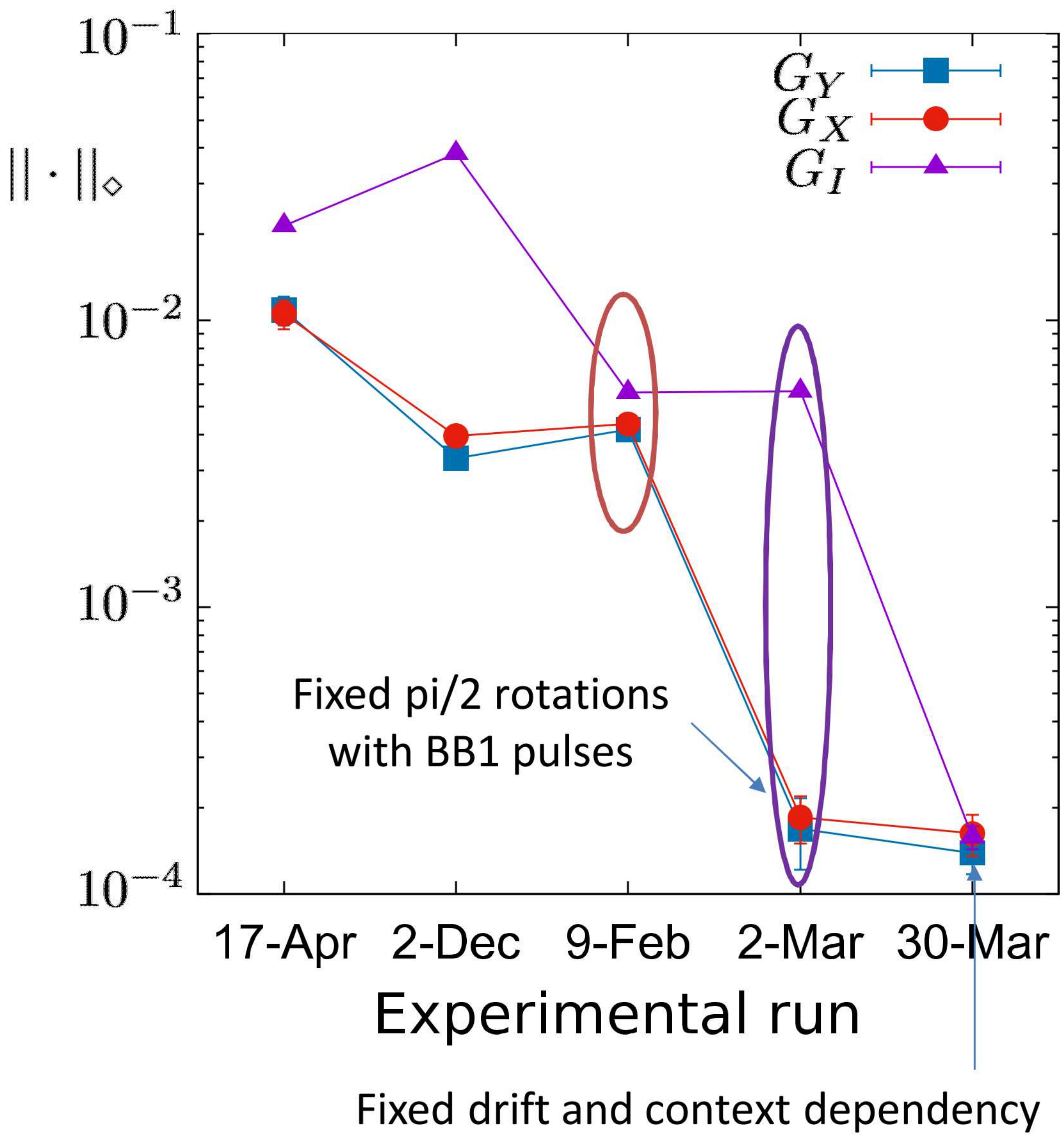

Single-Qubit GST Results

- Process infidelity ≈ diamond norm
  - This indicates that we have gotten rid of all systematic errors

Below the threshold for fault-tolerant error correction!

See P. Aliferis and A. W. Cross, Phys. Rev. Lett. 98, 220502 (2007)

- Co-propagating gates have infidelity comparable to microwave gates, but diamond norm indicates some residual control errors

- Counter-propagating gates are noticeably worse, but are necessary for two-qubit gates
- Lower fidelity presumably results from anomalous heating and optical phase sensitivity

Microwave Gates

Gate	Process Infidelity	1/2 ◊-Norm
G_I	$6.9(6) \times 10^{-5}$	$7.9(7) \times 10^{-5}$
G_X	$6.1(7) \times 10^{-5}$	$7.0(15) \times 10^{-5}$
G_Y	$7.2(7) \times 10^{-5}$	$8.1(15) \times 10^{-5}$

Laser Gates

co-propagating

Gate	Process Infidelity	1/2 ◊-Norm
G_I	$1.17(7) \times 10^{-4}$	$5.3(2) \times 10^{-4}$
G_X	$5.0(7) \times 10^{-5}$	$3(6) \times 10^{-4}$
G_Y	$6.9(6) \times 10^{-5}$	$4(9) \times 10^{-4}$

counter-propagating

Gate	Process Infidelity	1/2 ◊-Norm
G_I	$11.1(6) \times 10^{-4}$	$22.8(1) \times 10^{-4}$
G_X	$4.0(4) \times 10^{-4}$	$13.2(6) \times 10^{-4}$
G_Y	$4.1(4) \times 10^{-4}$	$8.4(8) \times 10^{-4}$

Two-Qubit Gate

- Bichromatic entangling "Mølmer-Sørensen" gate
- Gate time and detuning from motional sidebands is set so that population in motionally (de-)excited states is zero corresponding to a closed loop in phase space
- Does not require ground state cooling
- Requires a number of extra calibrations
    - Rabi frequencies of red/blue detuned transitions matched
    - Ions need to be evenly illuminated
    - Phase of beat note needs to be calibrated and stable

$$|00\rangle \rightarrow |00\rangle + |11\rangle$$

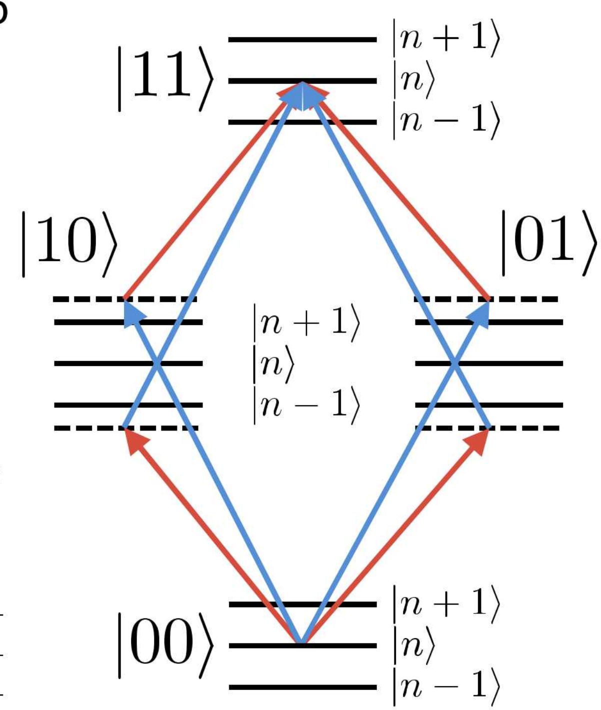

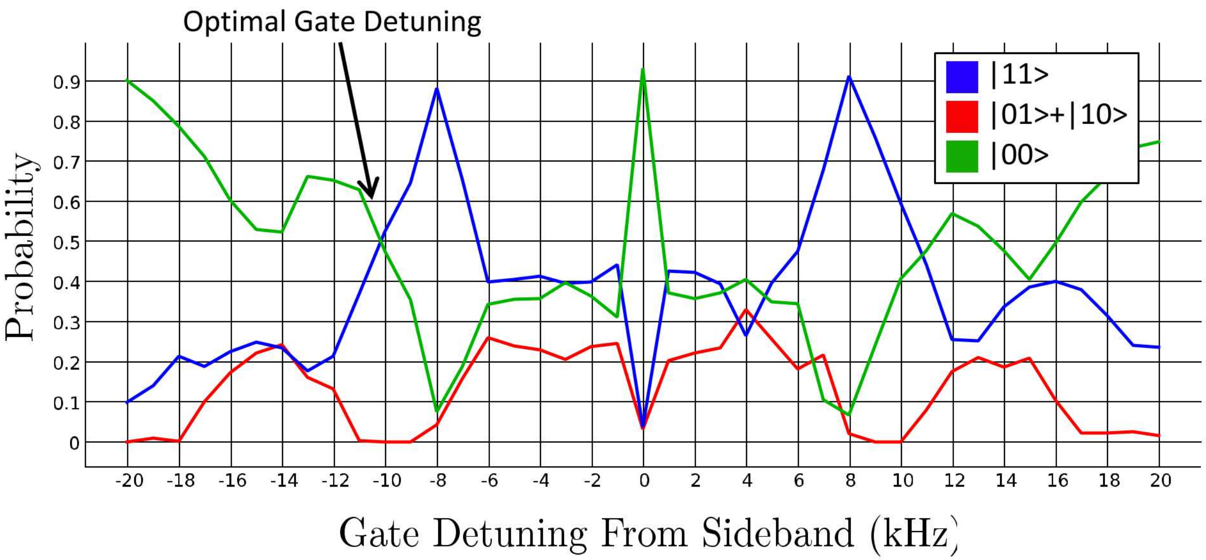

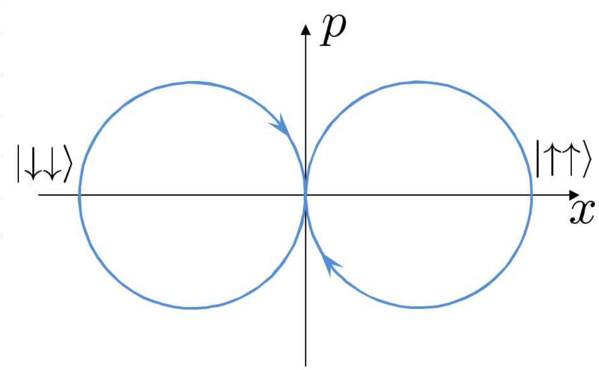

Characterizing the Mølmer-Sørensen Gate

Typical Approach: <u>Entangled State Fidelity</u>

- Entangled state fidelity determined by

$$\mathcal{F} = \underbrace{\frac{1}{2}\left(P(|00\rangle) + P(|11\rangle)\right)} + \underbrace{\frac{1}{4}c}$$

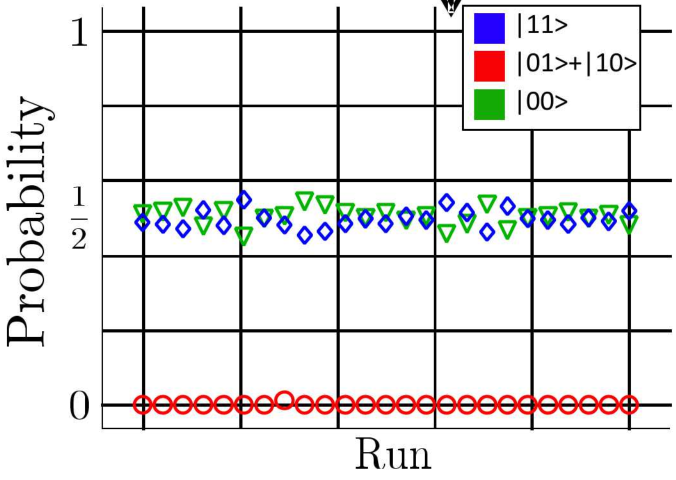

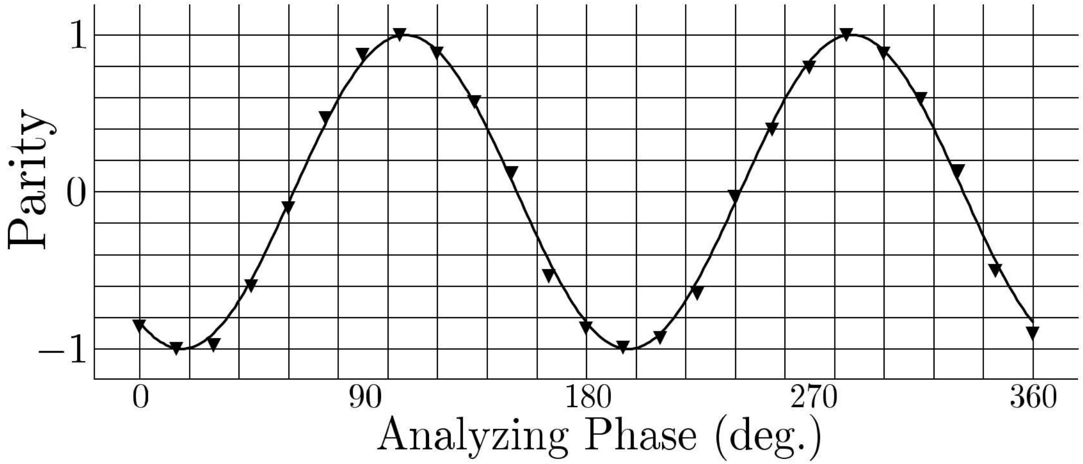

- Repeated application of gate
- Measure average population of entangled state

- Apply gate followed by analyzing pulse of varying phase
- Measure the resulting contrast

Two-Qubit GST

Typical Approach: Entangled State Fidelity

$$\mathcal{F} = \frac{1}{2}\left(P(|00\rangle) + P(|11\rangle)\right) + \frac{1}{4}c \approx 0.995$$

Two-Qubit GST

- Provides a true *process* fidelity
- Requires an extremely stable gate to take long GST measurements without constant recalibration
- Currently limited to the symmetric subspace

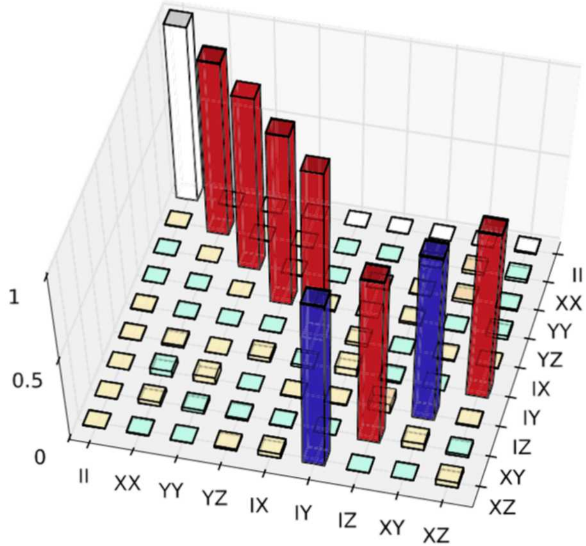

Gate	Process infidelity	$\frac{1}{2}$ Diamond norm
G_I	$1.6 \times 10^{-3} \pm 1.6 \times 10^{-3}$	$28 \times 10^{-3} \pm 7 \times 10^{-3}$
G_{XX}	$0.4 \times 10^{-3} \pm 1.0 \times 10^{-3}$	$27 \times 10^{-3} \pm 5 \times 10^{-3}$
G_{YY}	$0.1 \times 10^{-3} \pm 0.9 \times 10^{-3}$	$26 \times 10^{-3} \pm 4 \times 10^{-3}$
G_{MS}	$4.2 \times 10^{-3} \pm 0.6 \times 10^{-3}$	$38 \times 10^{-3} \pm 5 \times 10^{-3}$

95% confidence intervals

$$F_{MS} = 0.9958(6)$$

$$\frac{1}{2}||G_{MS}||_{\diamond} = 0.08(1)$$

- Much more rigorous characterization
- Gate is stable for several hours

Outline

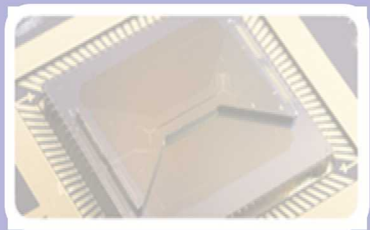

Sandia's High-Optical-Access Trap

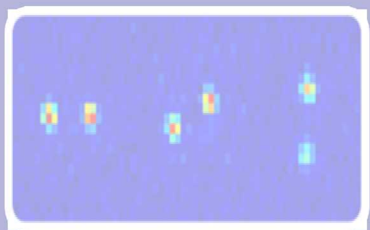

Classical Control

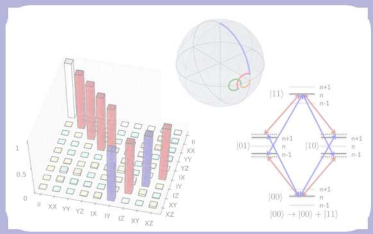

Quantum Control

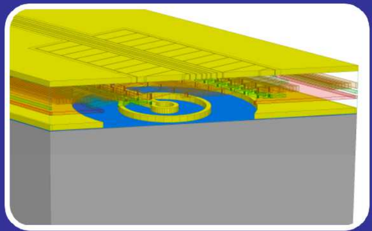

Specialized Ion Traps

Microwave Surface Trap

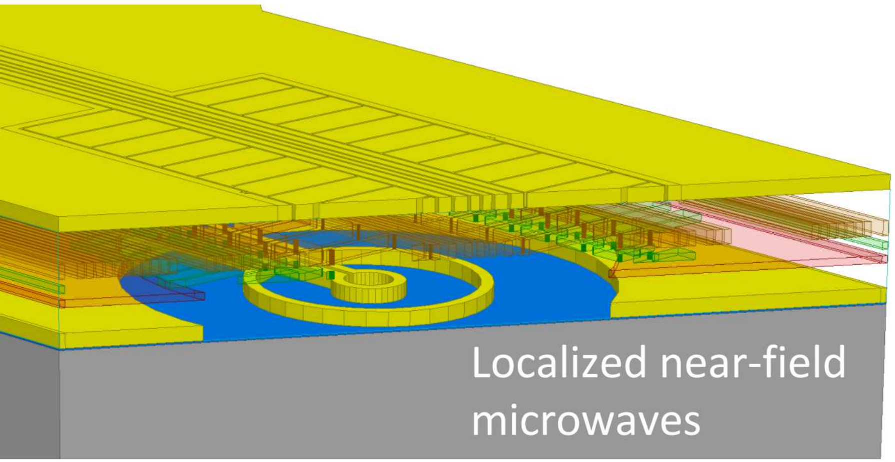

Benefits:

- Microwave radiation is easier to control and cheaper to implement than lasers
- Low power for Rabi oscillations
- Near field allows to generate microwave gradient fields

Challenges:

- Microwave delivery
- Dissipation, heating, thermal management

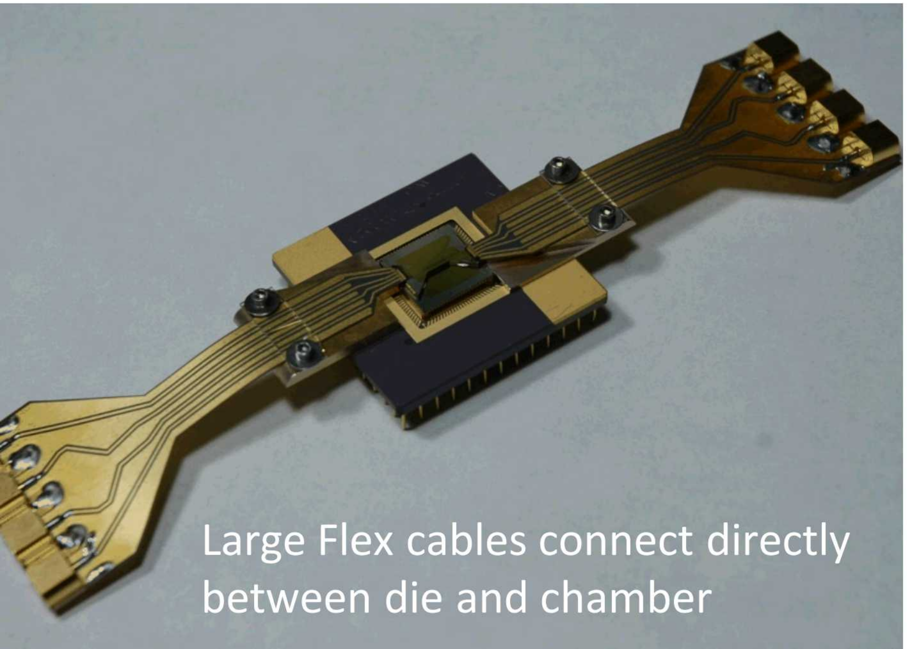

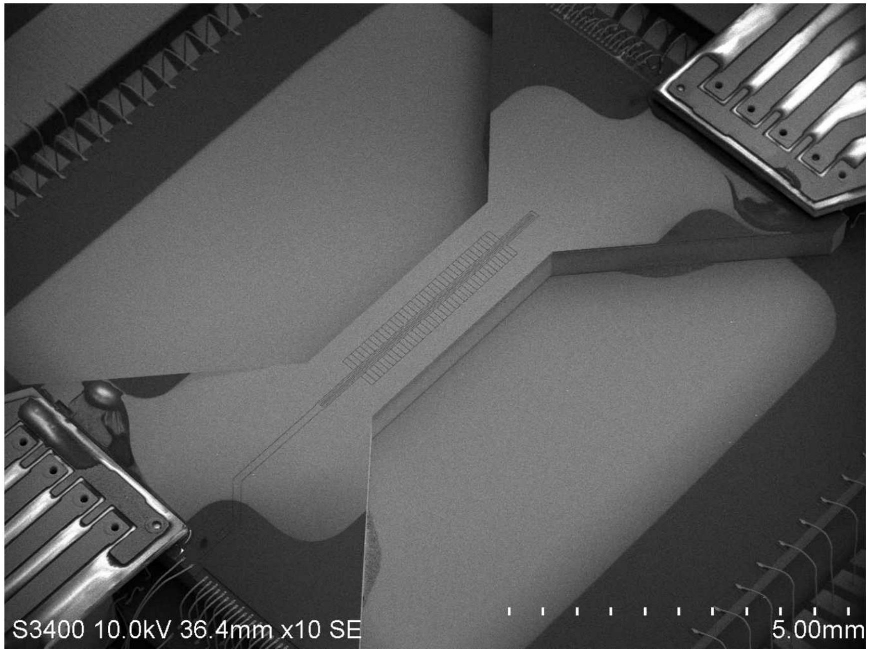

Microwave Magnetic Fields

Two-Current Loop Design

"Ideal" Two-Loop Design

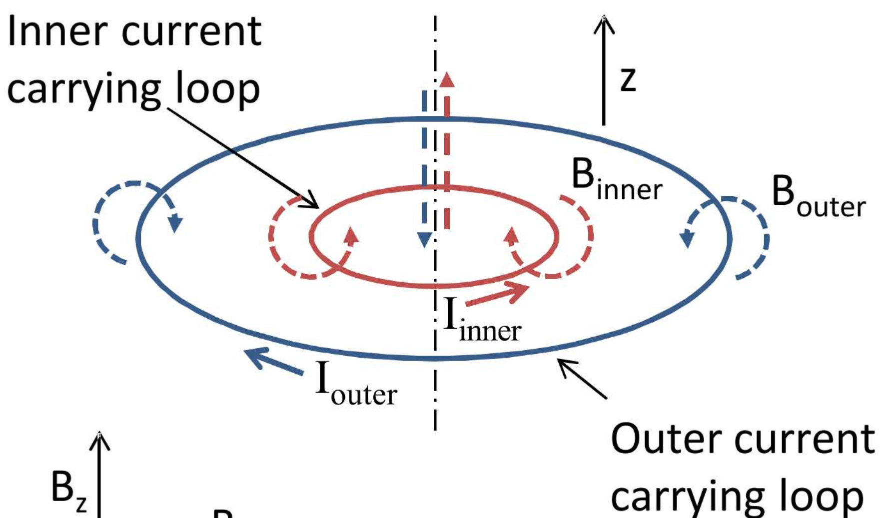

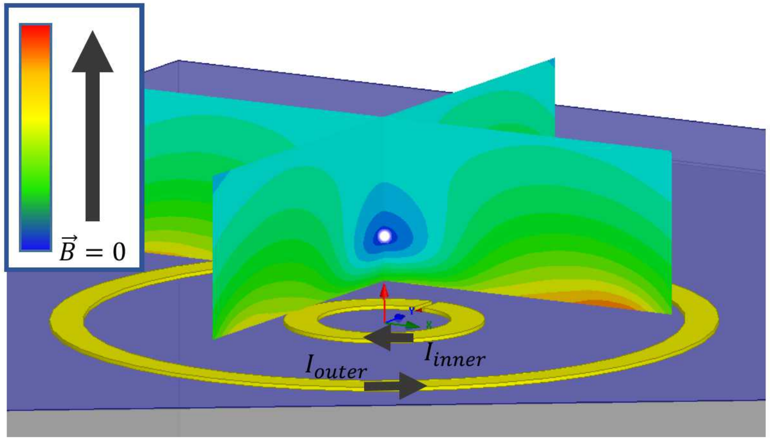

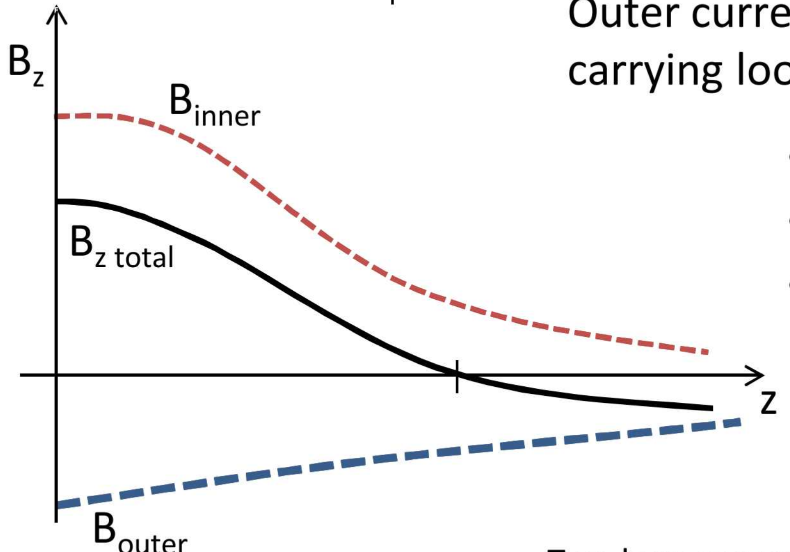

- x- and y- fields cancel along z-axis
- Generates uniform B_z and dB_z/dz with B=0
- Location of null determined by geometry and ratio of currents

Two-loop concept developed at Sandia in 2012 (SAND2015-9513)
(C. Highstrete, S. M. Scott, J. D. Sterk, C. D. Nordquist, J. E. Stevens, C. P. Tigges, M. G. Blain)

Microwave trap
Rabi oscillations

- Losses between chamber and device ≈17dB
- Realized fast Rabi flopping 330ns with 15dBm at chamber, -2dBm at device
- Access to range of relevant π-times
- Will characterize gates as function of π-times.

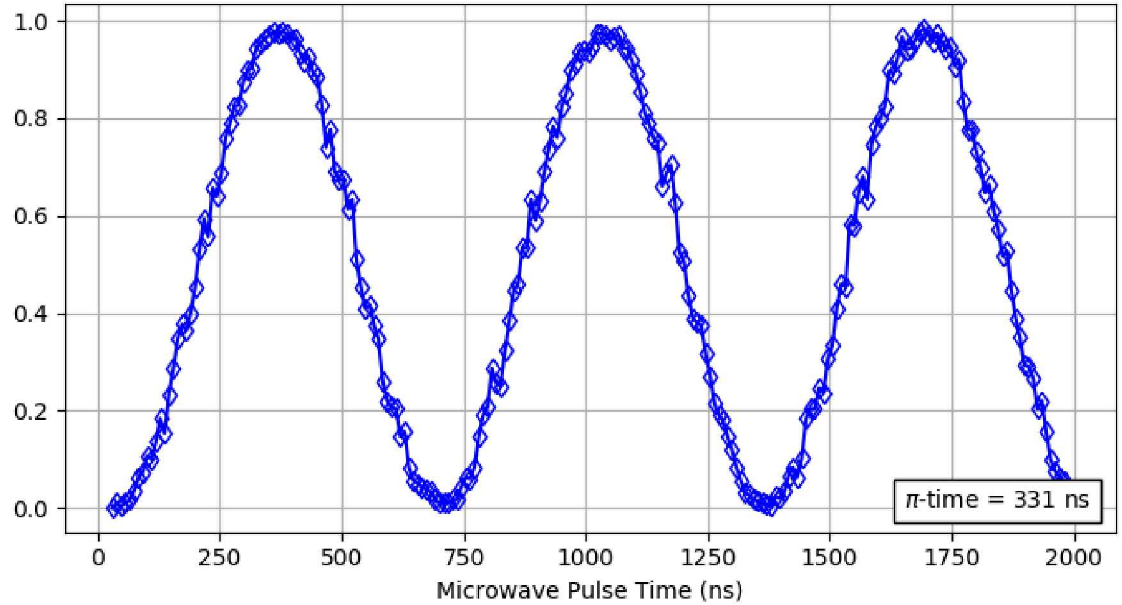

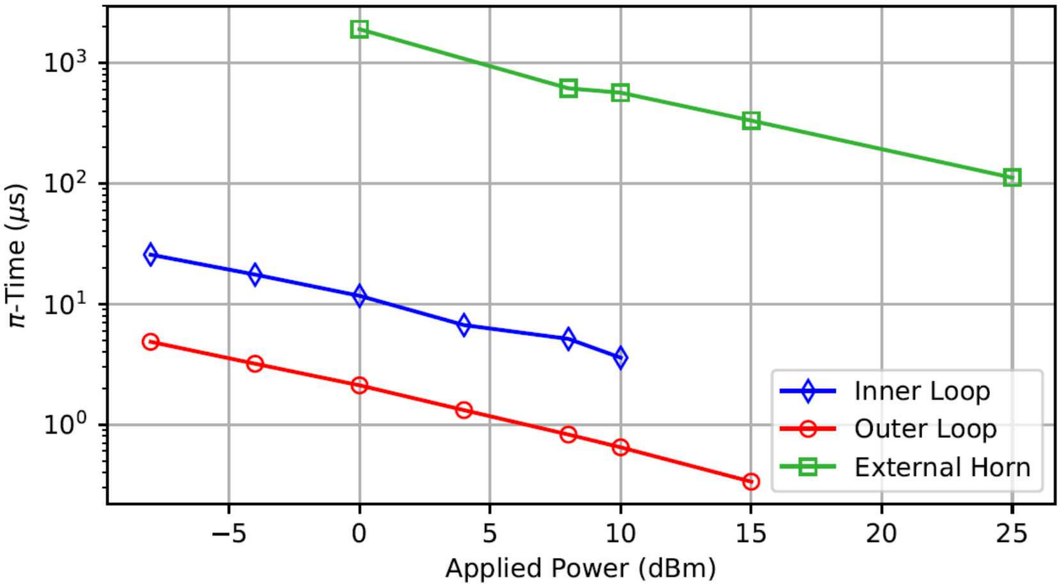

EPICS Trap

- Integrated Superconducting Nanowire Single-Photon Detector (SNSPD) detector and reflective backplane
  - Detector developed by JPL/NIST
- SNSPD provides higher photon detection (>80% vs <30%)
- Cavity-QED provides higher photon collection efficiency
- Strong coupling regime enables qubit measurement via fast cavity transmission
- Extra rf electrodes enable alignment of rf node with cavity modes

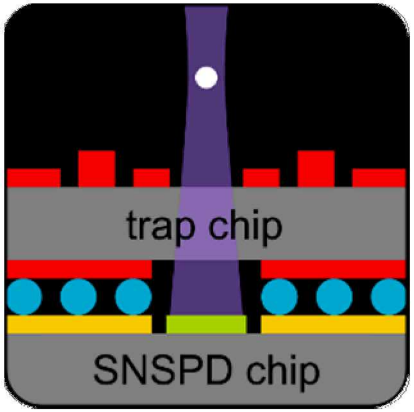

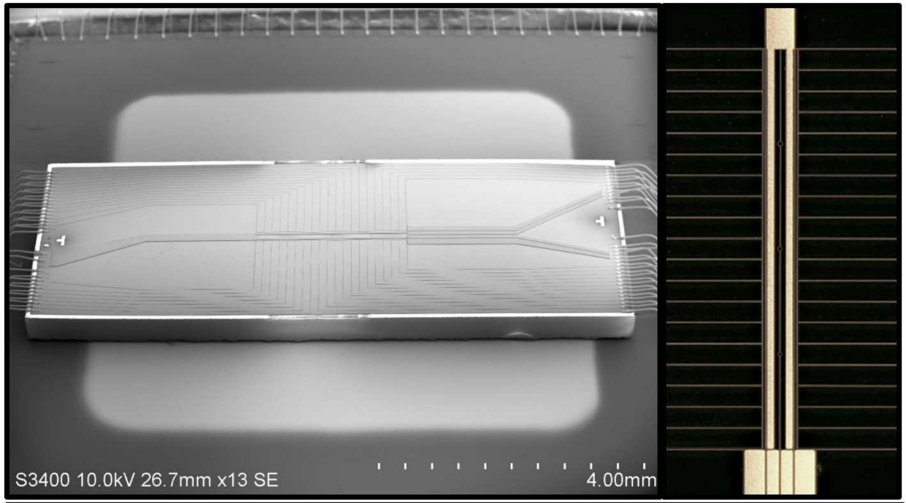

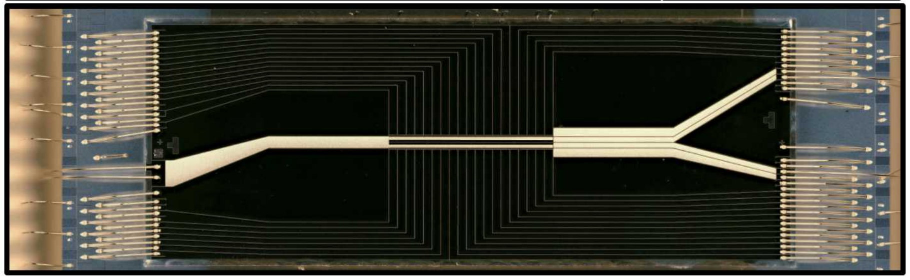

Ion Trap Fabrication (Duke/SNL)

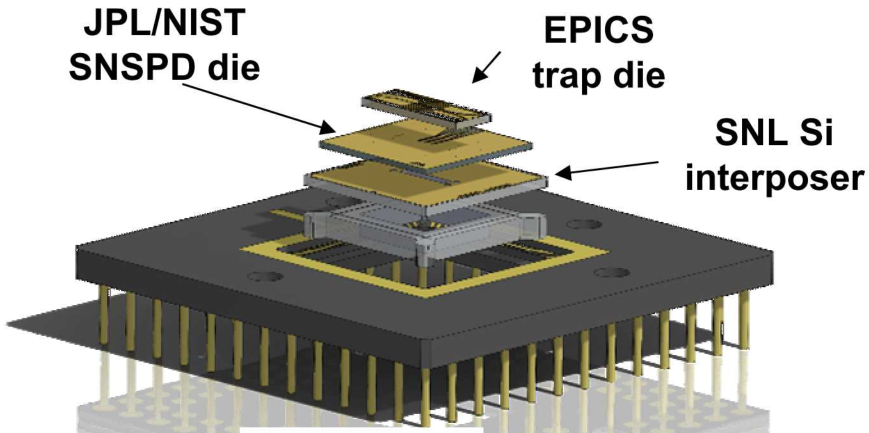

collaboration with NIST National Institute of Standards and Technology U.S. Department of Commerce, JPL Jet Propulsion Laboratory, Duke University

EPICS Trap

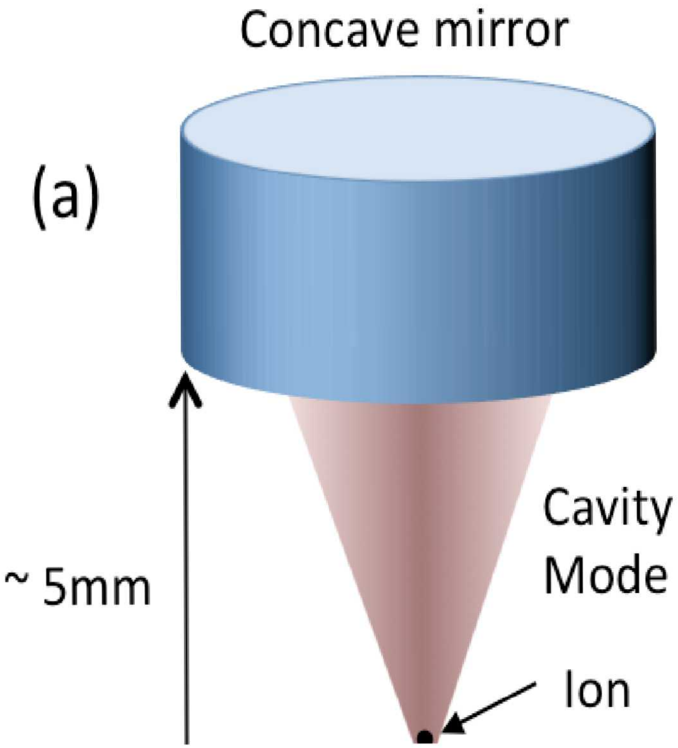

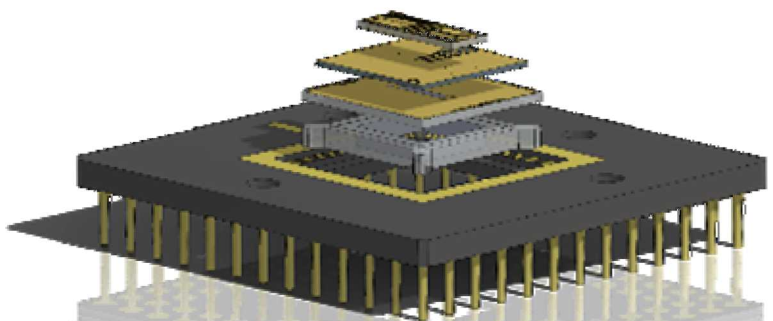

(b

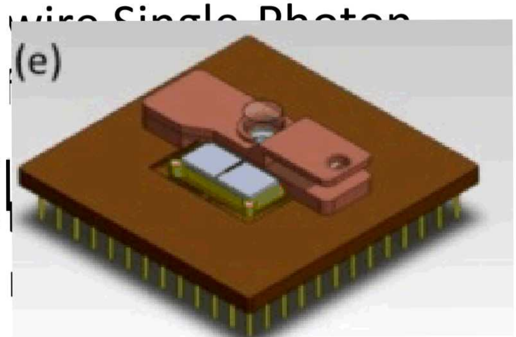

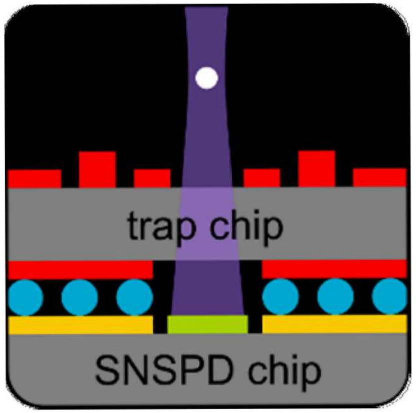

ent

i

ser

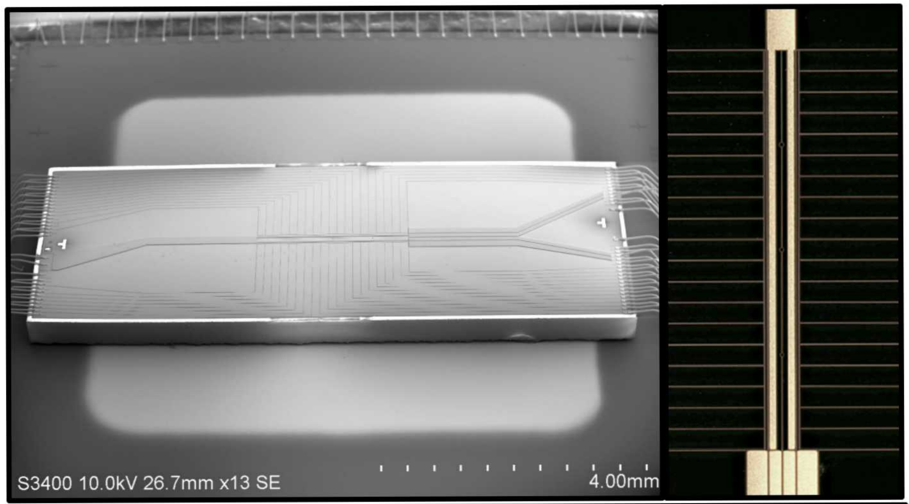

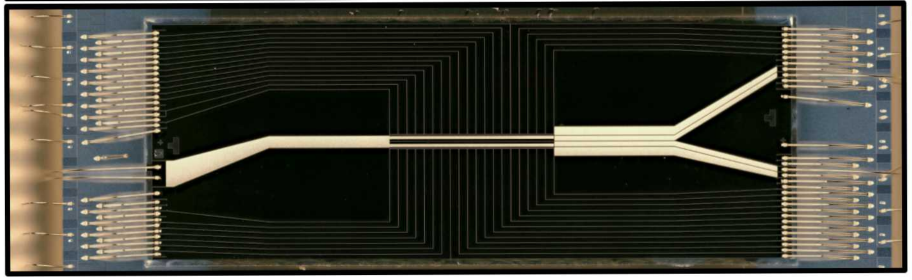

collaboration with

Thank you

Trap design fabrication
Matthew Blain
Ed Heller
Corrie Herrmann
Becky Loviza
John Rembetski
Paul Resnick
SiFab team

Trap packaging
Ray Haltli
Drew Hollowell
Anathea Ortega
Tipp Jennings

Trap design and testing
Peter Maunz
Craig Hogle
Daniel Lobser
Melissa Revelle
Dan Stick
Christopher Yale

RF Engineering
Christopher Nordquist
Stefan Lepkowski

GST protocols
Robin Blume-Kohout
Kenneth Rudinger
Eric Nielsen

Coming Soon:
Quantum Scientific Open User Testbed (QSCOUT)

- Quantum processor with 5 – 15 qubits
- Realized in trapped ion technology

Features
- Low single and two qubit error rates ($<10^{-4}$, $<2 \times 10^{-2}$)
- All to all connectivity between qubits
- Random algorithm execution capability
- Access to all relevant low-level implementation details
- Capability to change low-level gate implementation

User support
- Exemplar programs and demonstrations
- User workshops and conferences (together with LBNL)

Availability
- Available to the DOE Scientific computing community
- First device will come online at end of 2019

Postdocs wanted!

Apply @ https://sandia.gov/careers
→ View All Jobs → Search "665253"
Questions? dlobser@sandia.gov

Motivation

Quantum Information

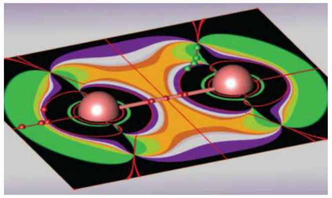

Quantum chemistry
- Calculation of molecular potentials
- Nitrogen and Oxygen fixation, development of catalytic converters

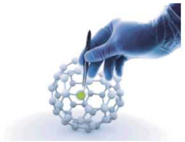

Medicine
- Structure-based drug development

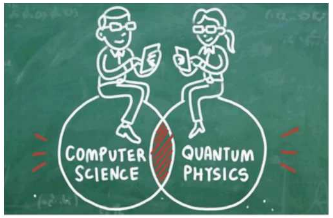

Quantum computing
- Number factorization (Shor's algorithm)
- Search in unstructured data, searching for solutions to hard problems (Grover's search algorithm)

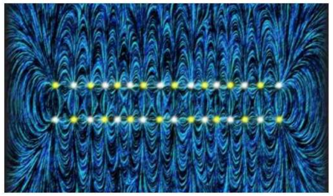

Quantum simulation
- Simulating many-body systems
- Already for about 20 qubits not possible to simulate classically.

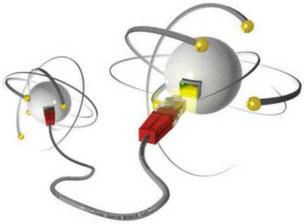

Quantum Communication
- Securing a quantum channel

Qubit Implementations

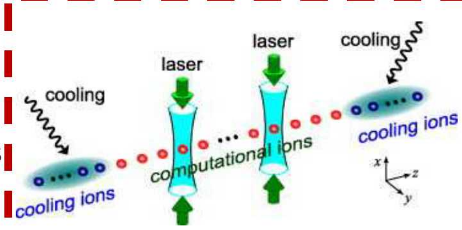

Trapped Ions
- Blatt and Wineland "Entangled States of Trapped Atomic Ions." *Nature* 453, 1008–15 (2008).
- Monroe and Kim. "Scaling the Ion Trap Quantum Processor." *Science* 339, 1169 (2013).

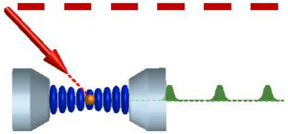

Neutral Atoms
- Rydberg states
- Atoms in cavities

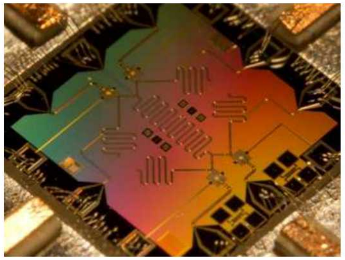

Superconducting Josephson junctions
- Devoret and Schoelkopf. "Superconducting Circuits for Quantum Information: An Outlook." *Science* 339, 1169 (2013).

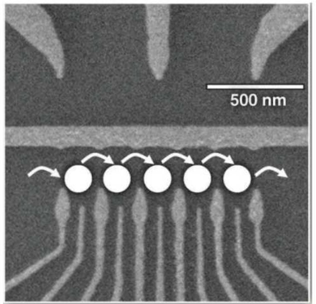

Quantum dots
- Awschalom, et al., "Quantum Spintronics: Engineering and Manipulating Atom-Like Spins in Semiconductors." *Science* 339, 1174 (2013).

Brief Overview of Ion Trapping

Earnshaw's Theorem: *Static electric fields can't create a stable confining potential for charged particles*

r.f. Paul Trap

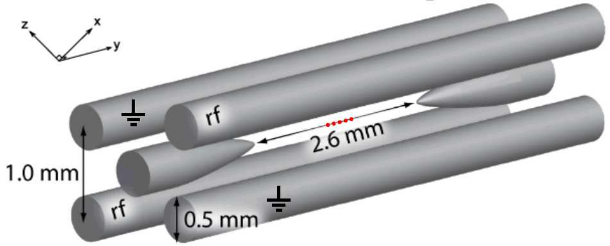

r.f. pseudopotential

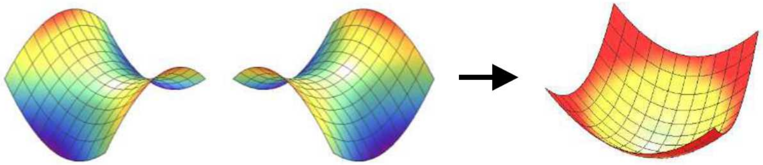

- Time-averaged potential is close to harmonic at the saddle point
- Off the saddle point, ions experience micromotion
- Works well for linear chains of ions
- Doesn't support fine control of ion position or confining potential

Segmented Paul Trap

- Better control over confining potential
- Difficult to construct
- Doesn't scale well

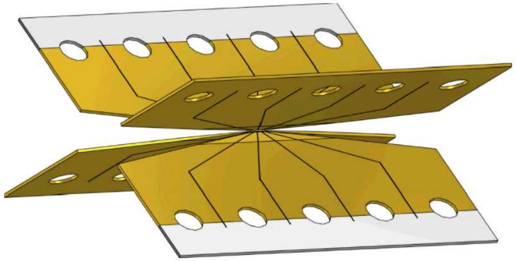

Microfabricated Surface Trap

- Consistent, well-defined electrode layout
- Microfabrication supports a lot of exotic electrode geometries
- Excellent control over potential
- Very scalable

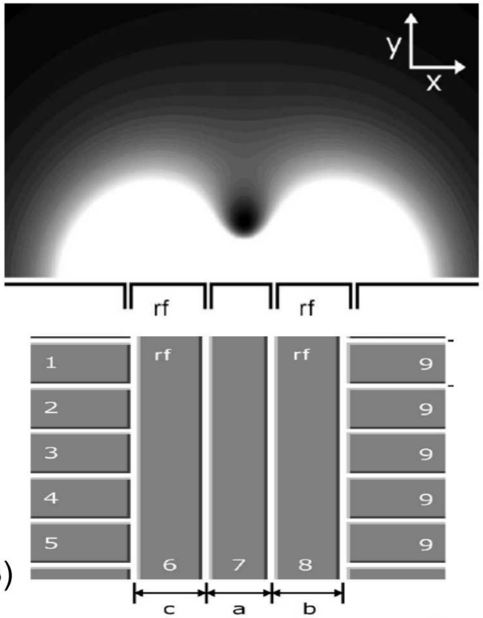

House, PRA **78** 033402 (2008)

Measuring swap fidelity

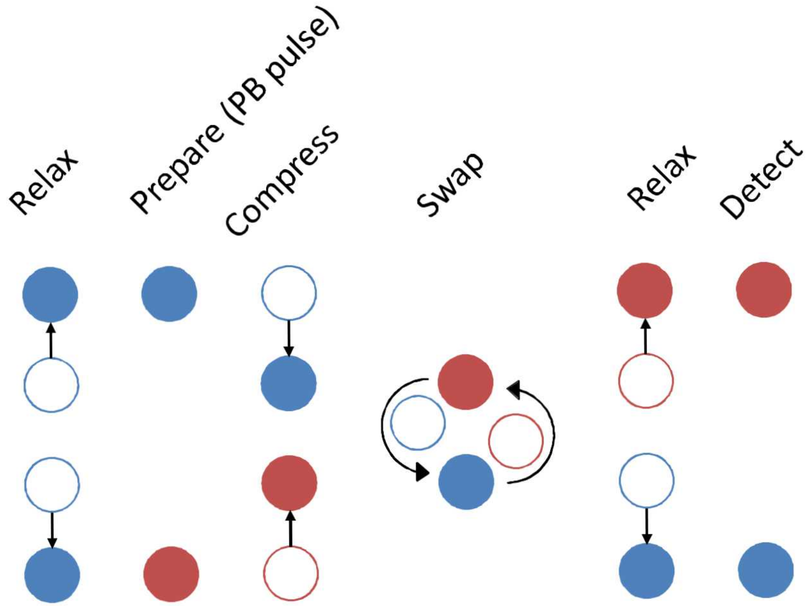

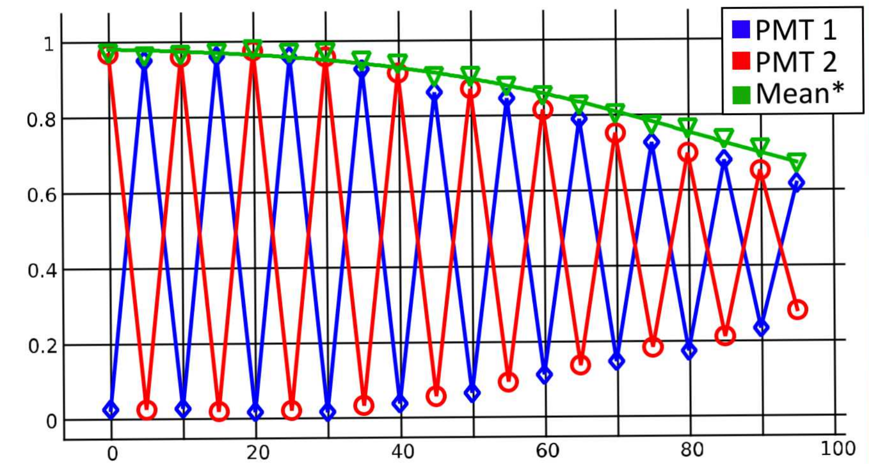

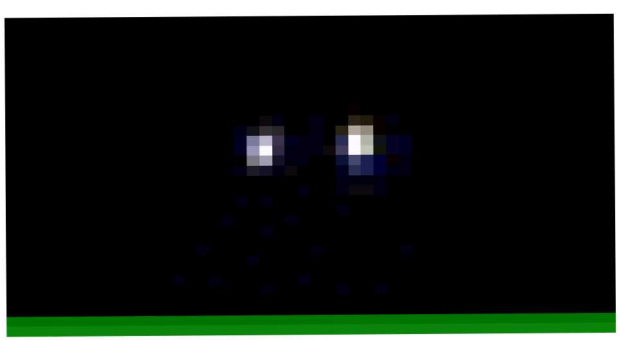

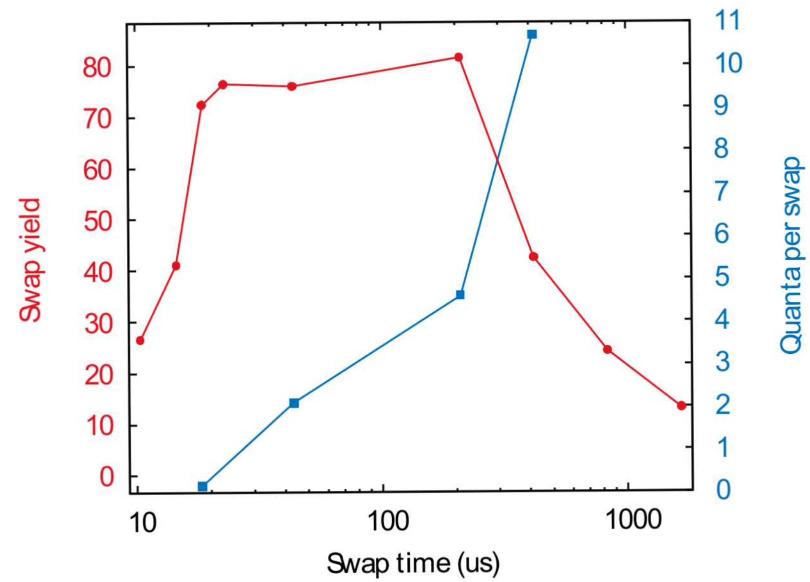

Swap verification

- Displacing the Raman beam leads to disparate Rabi frequencies
- Contrast is improved by using PB1 compensated pulses

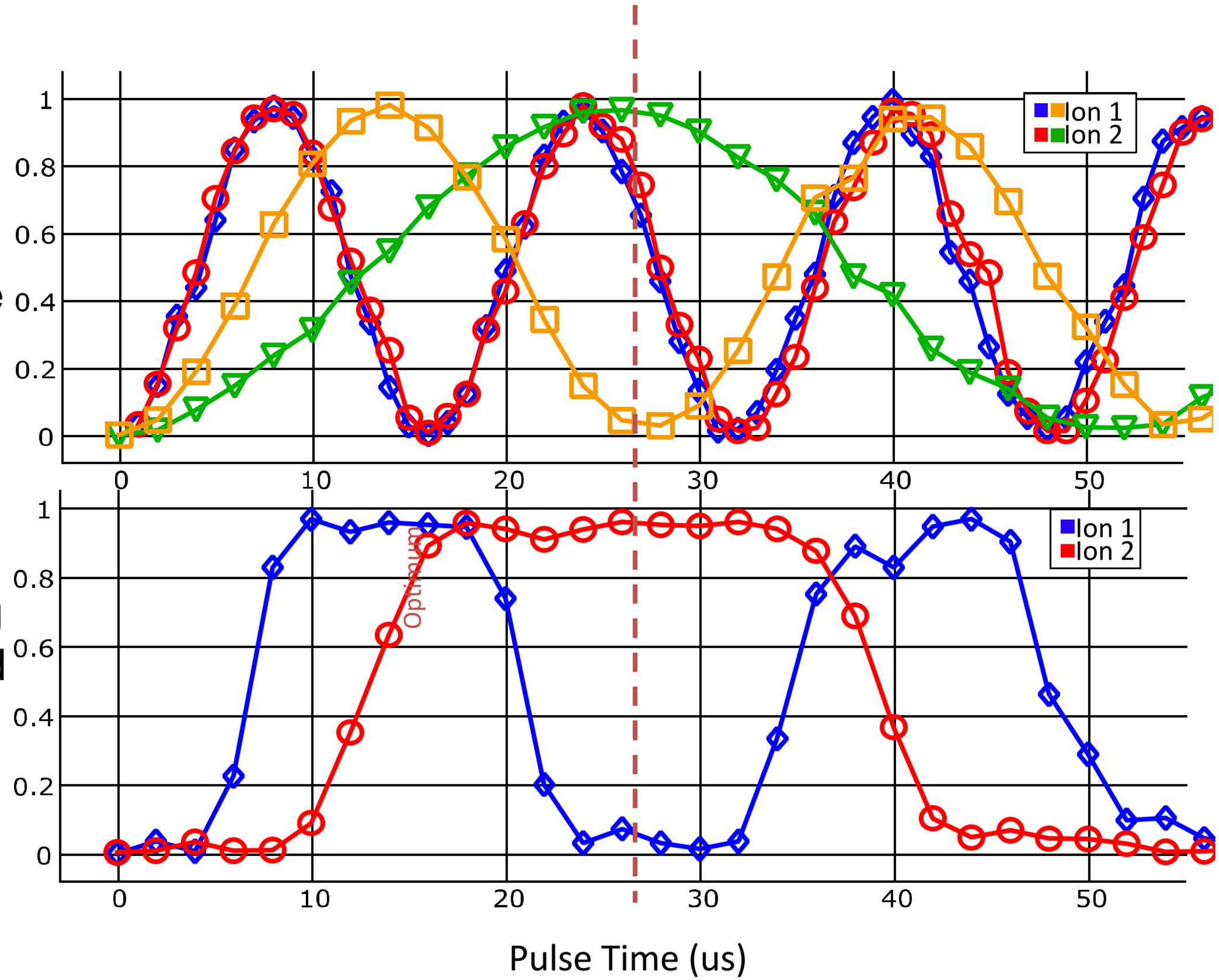

Swap breakdown

- The absolute upper bound on velocity for a successful swap is limited by timing constraints
- Swaps degrade after multiple rotations
- Swap yield is determined by decay of the mean, given by (1-P(|0>)+P(|1>))/2

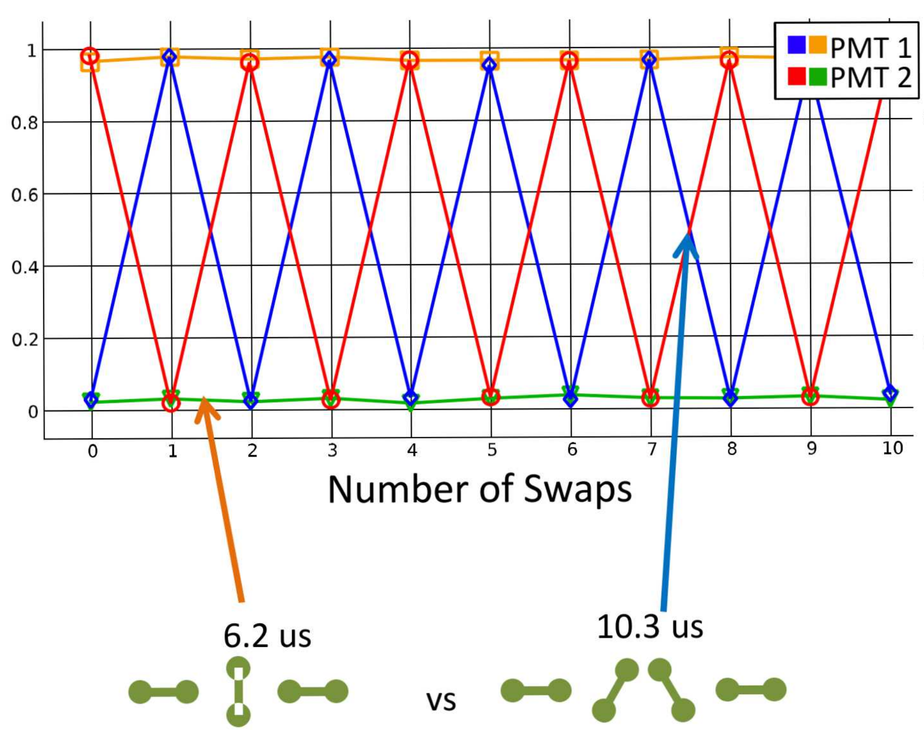

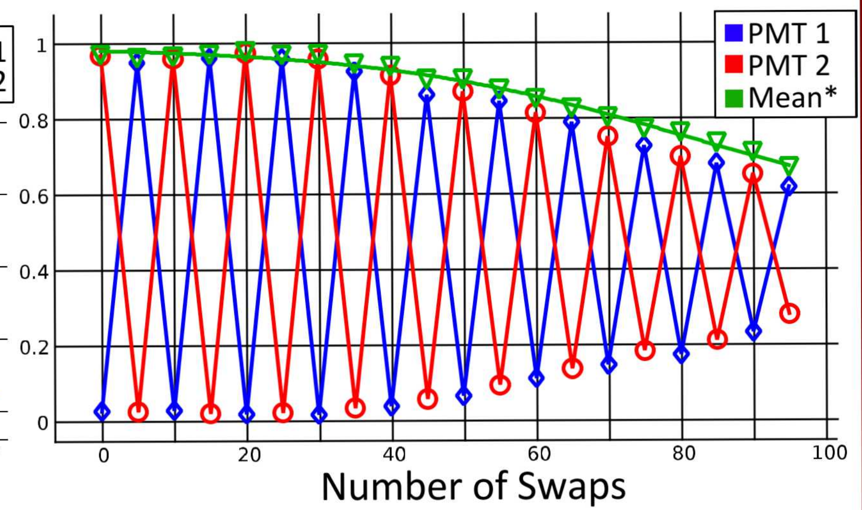

Capabilities & Requirements

Derived requirements

- Standardization (lithographically defined electrodes)
- Multi-unit production
- Multi-level lead routing for accessing interior electrodes
- Voltage breakdown >300 V @ ~50 MHz
- Overhung electrodes
- Low electric field noise (heating)
- Backside loading holes
- Trench capacitors
- High optical access (delivery and collection)

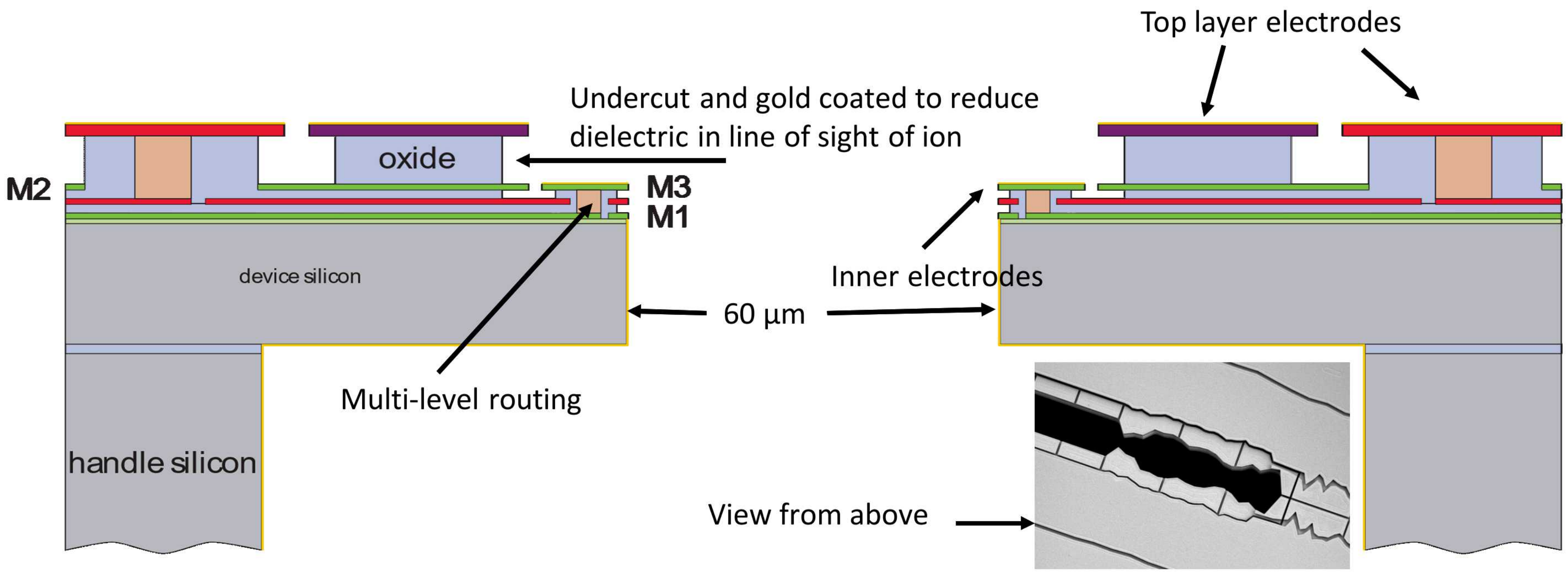

High Optical Access (HOA)

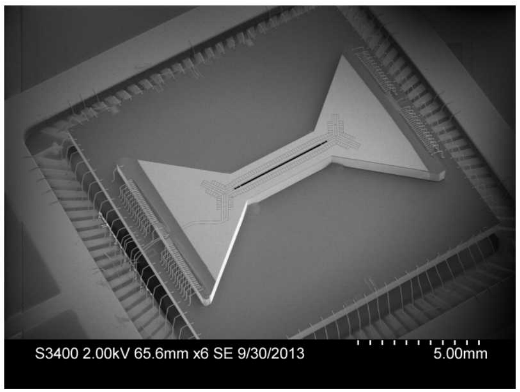

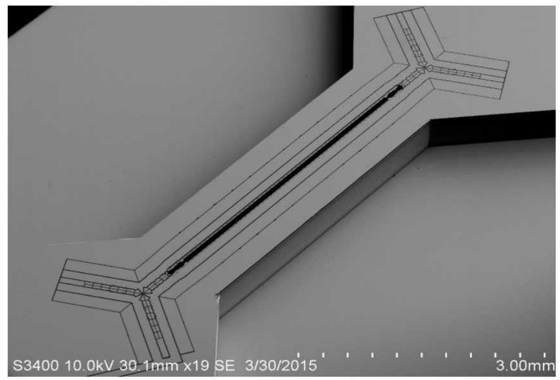

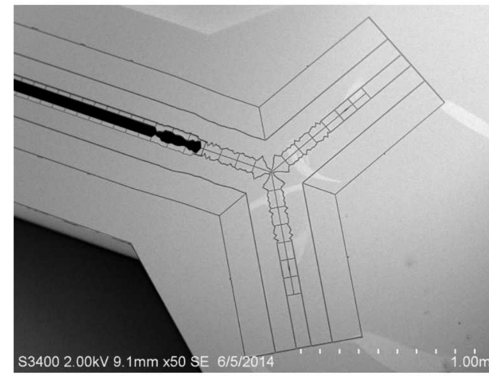

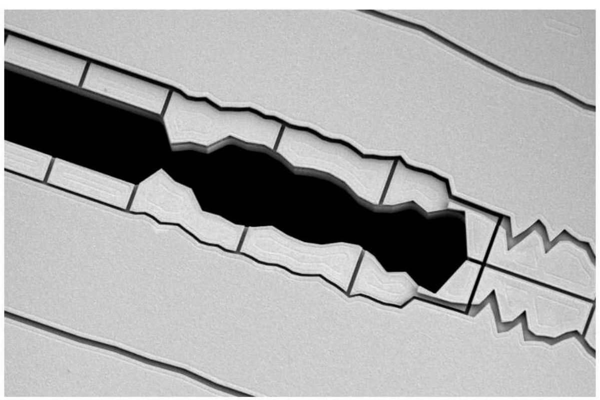

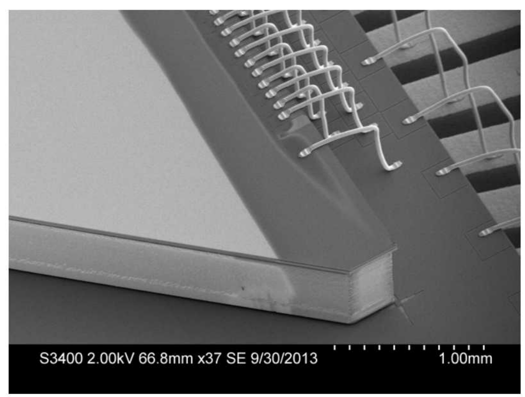

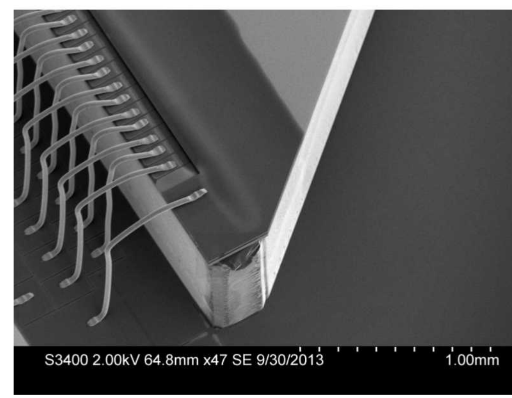

Shuttling Solutions

- Same method can be used along entire trap

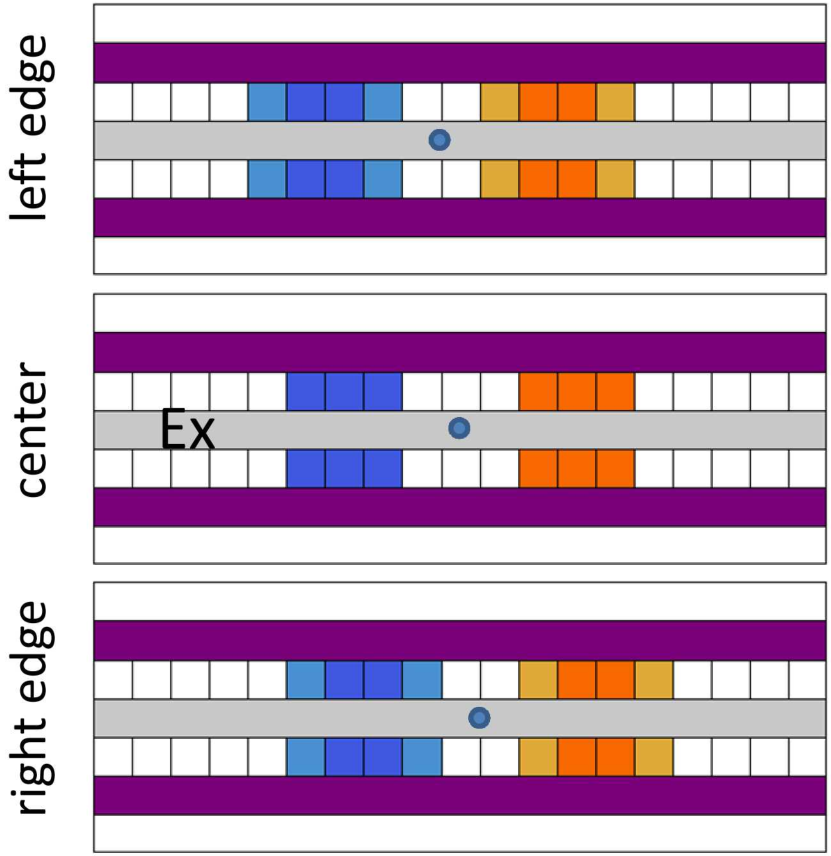

Solution for Ex field in increments of 5 um

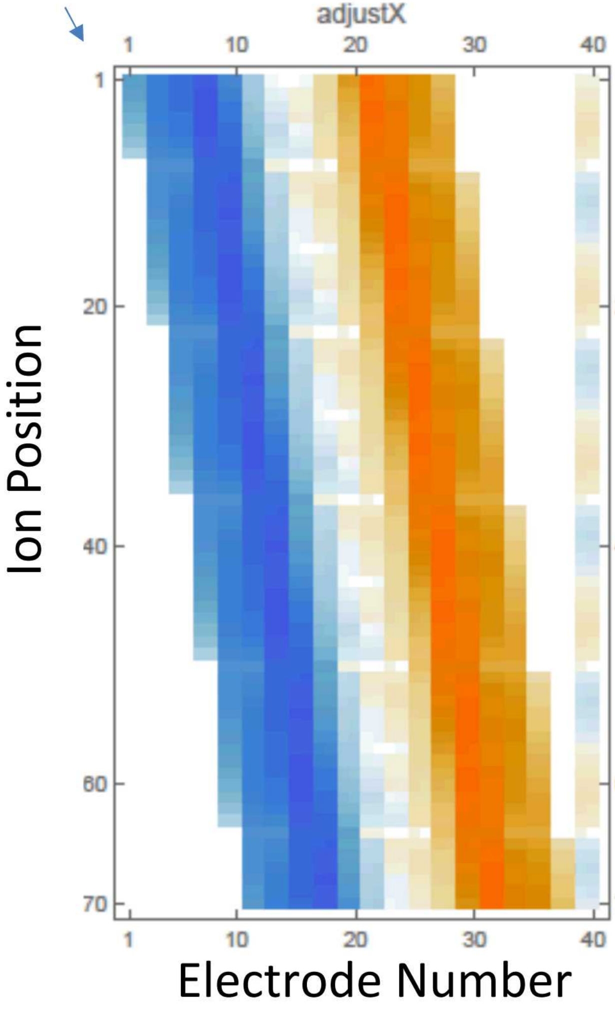

Shuttling Solutions

- Generate basis solutions for each point

Advantages:

- Solution are orthogonal

- Full parametric control over trap parameters at each point during shuttling

- Optimization techniques, such as machine learning or search algorithms, can be used to dynamically change basis amplitudes for improved shuttling

- Shuttling primitives can easily be decoupled, for example crystal rotation or linear shuttling at any position in the trap

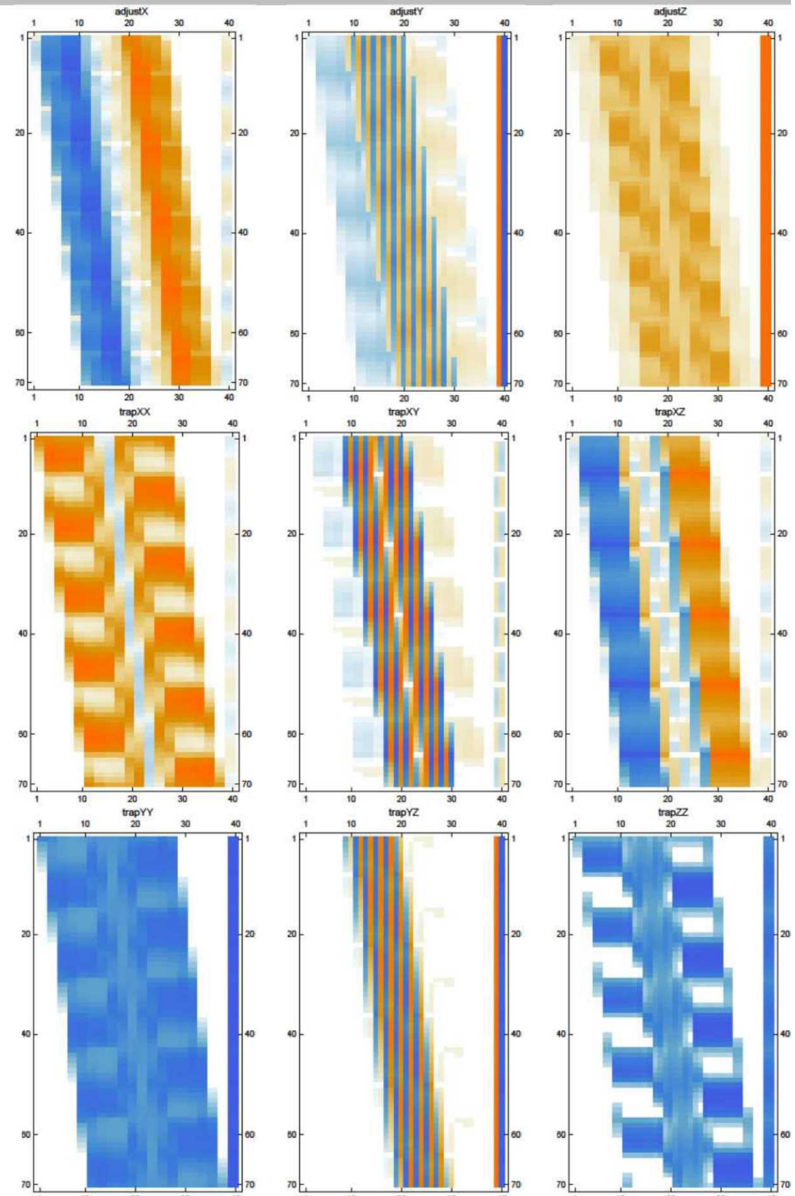

Trap frequency vs linear offset

- Trap frequencies are stable to within 16 kHz over the course of linear shuttling

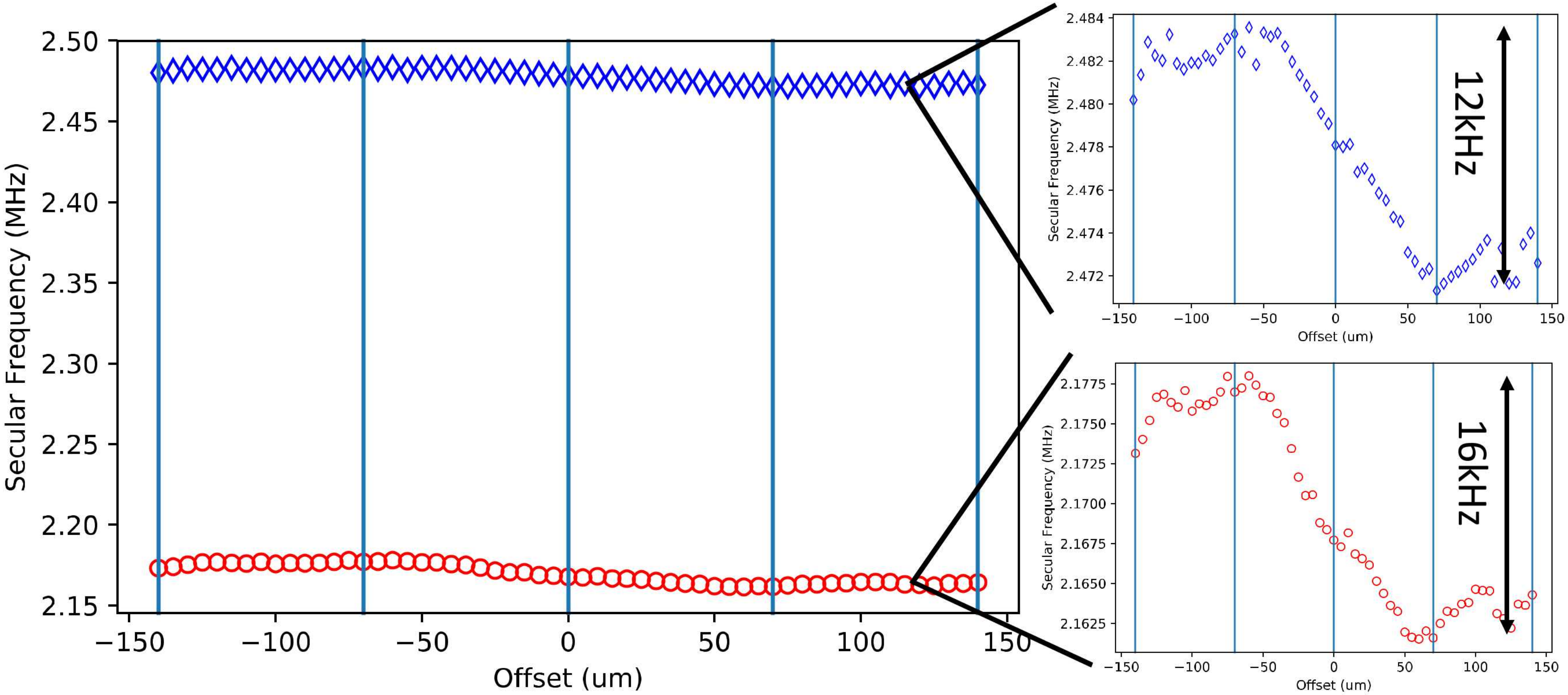

Optimization

- Shuttling in linear section over 140μm, 5 repeats
- Optimization performed with a Nelder-Mead type simplex algorithm

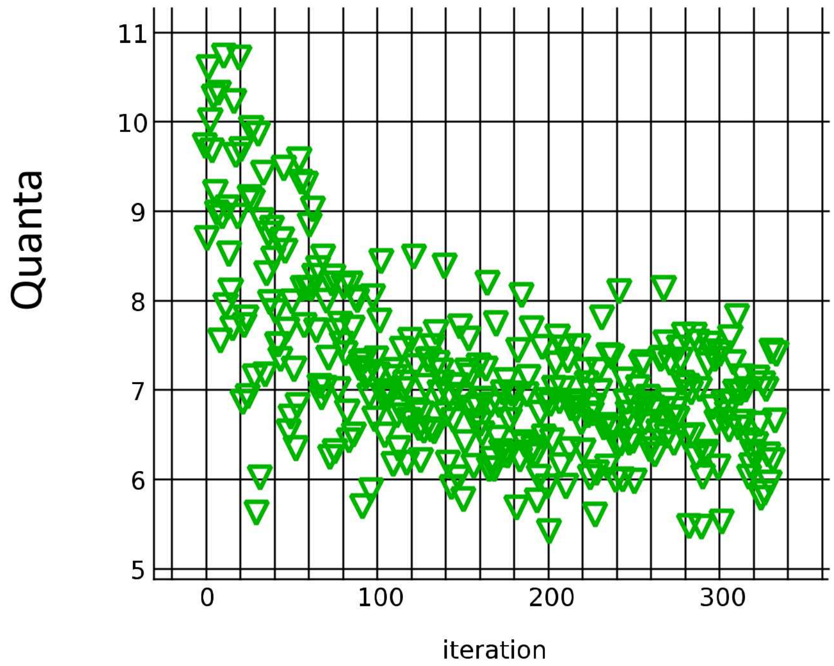

- 12 degrees of freedom for x, y, z offset fields

- First attempts at optimization demonstrate nearly a factor of 2 in heating rate during shuttling

Microwave trap properties

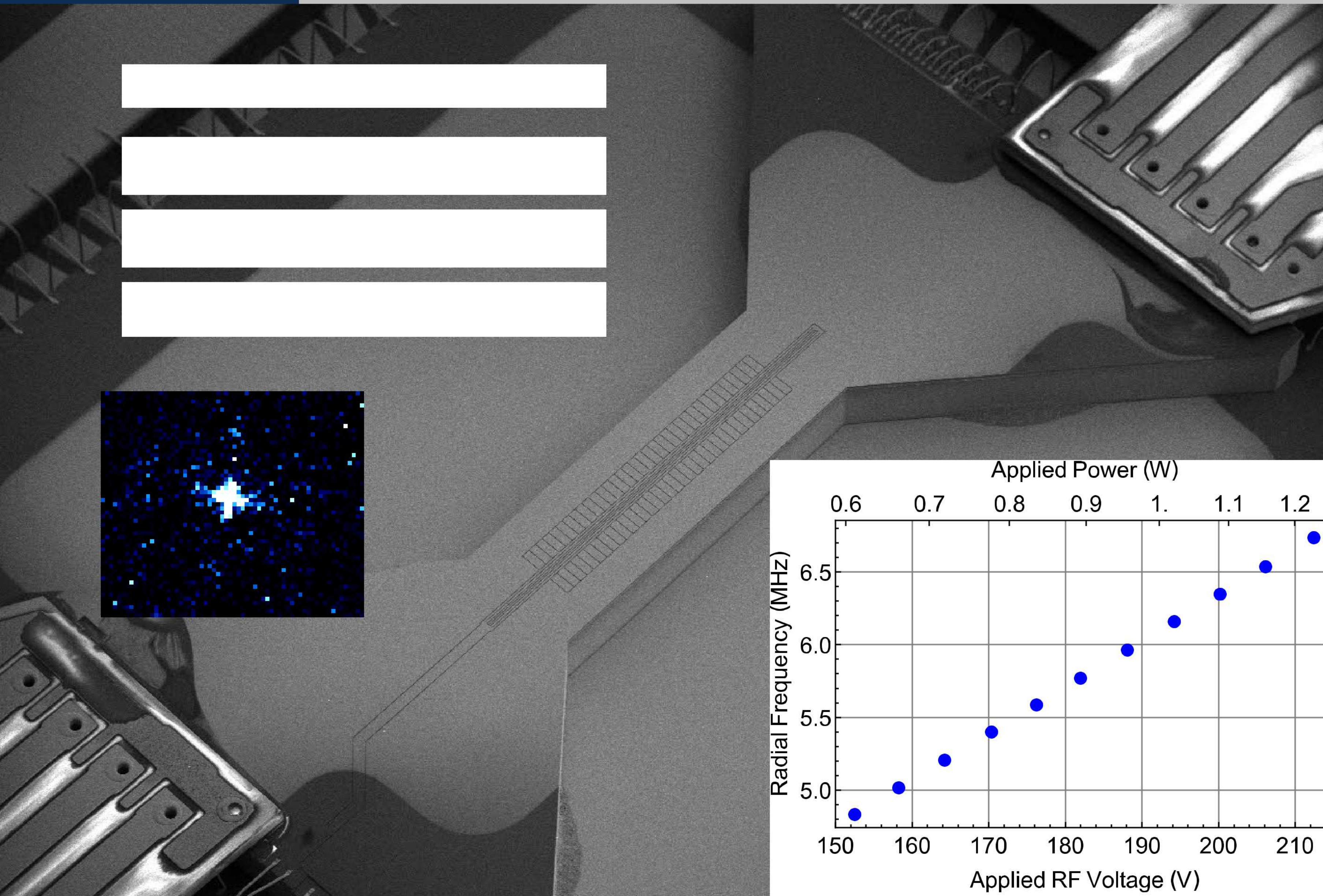

Two-qubit gate implementation

- Mølmer-Sørensen gates [1] using 355nm pulsed laser
- All two-qubit gates implemented using Walsh compensation pulses [2]

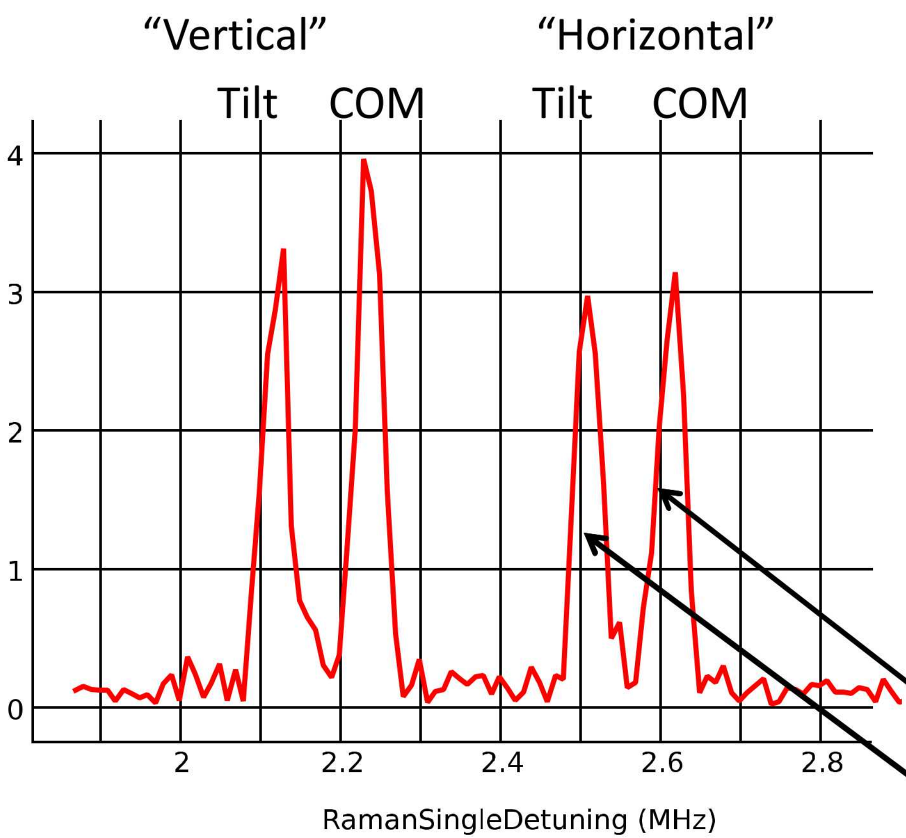

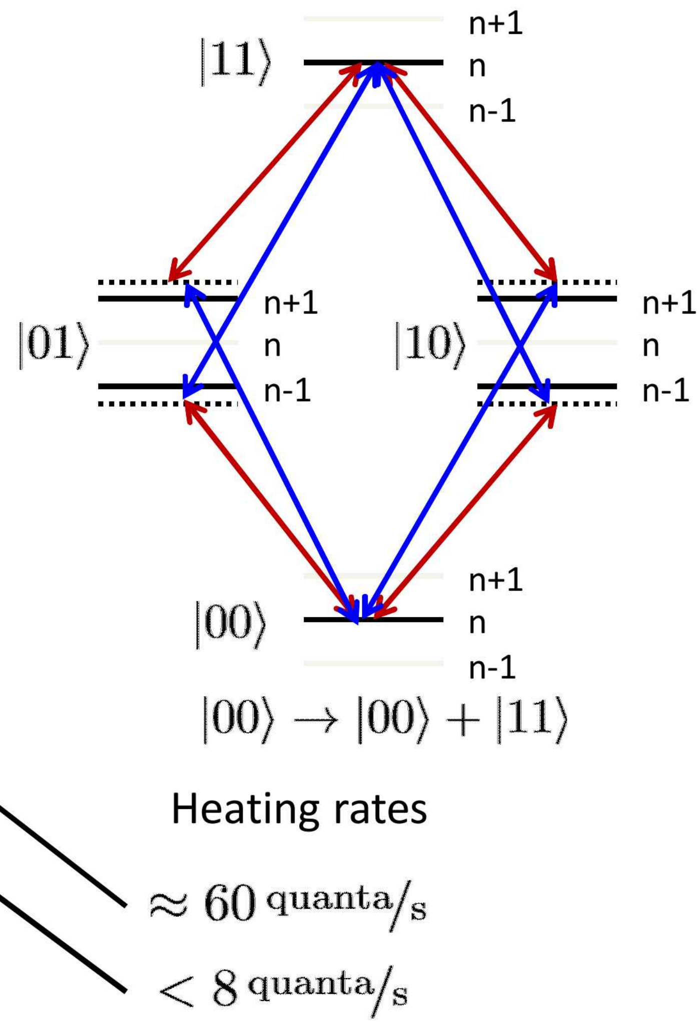

[1] K. Mølmer, A. Sørensen, PRL 82, 1835 (1999)
[2] D. Hayes et al. Phys. Rev. Lett. 109, 020503 (2012)

GST on symmetric subspace

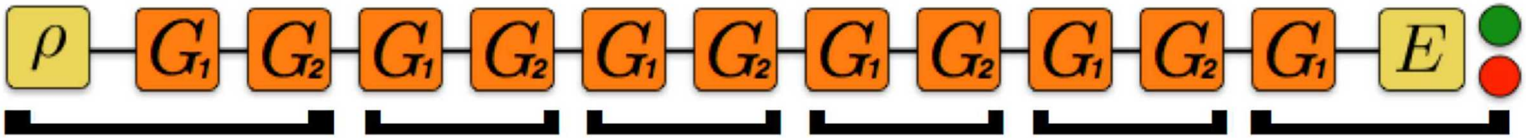

Basic gates:

$$G_I$$

$$G_{XX} = G_X \otimes G_X$$

$$G_{YY} = G_Y \otimes G_Y$$

$$G_{MS}$$

Preparation Fiducials:

$\{\}$

G_{XX}

G_{YY}

G_{MS}

$G_{XX}G_{MS}$

$G_{YY}G_{MS}$

Germs:

G_I

G_{XX}

G_{YY}

G_{MS}

$G_I G_{XX}$

$G_I G_{YY}$

$G_I G_{MS}$

$G_{XX}G_{YY}$

$G_{XX}G_{MS}$

$G_{YY}G_{MS}$

$G_I G_I G_{XX}$

$G_I G_I G_{YY}$

Detection Fiducials:

$\{\}$

G_{XX}

G_{YY}

G_{MS}

$G_{XX}G_{MS}$

$G_{YY}G_{MS}$

G_{XX}^3

G_{YY}^3

$G_{YY}^2 G_{MS}$

Scaling trapped ion systems

Quantum charge coupled device

Kielpinsky, Monroe and Wineland, *Nature* **417**, 709 (2002)

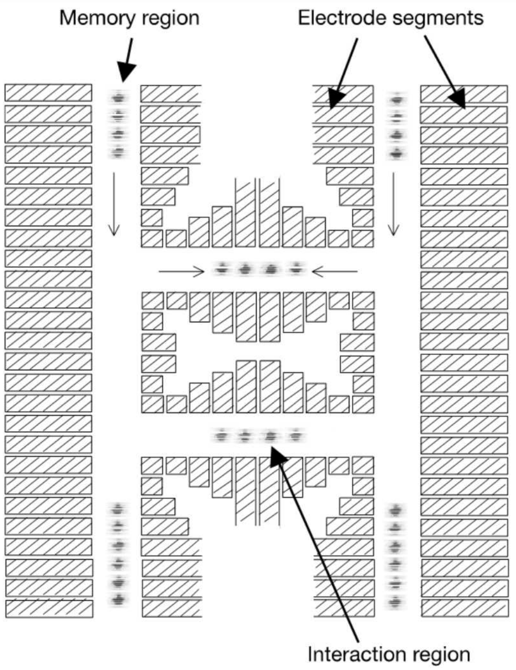

MUSIQC scaling (scaling beyond a single chip using remote entanglement)

Monroe, et al., *Physical Review A* 89, 022317 (2014).

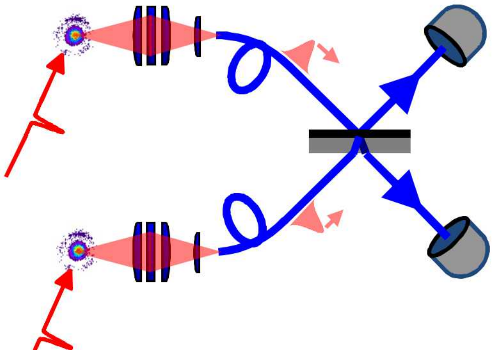

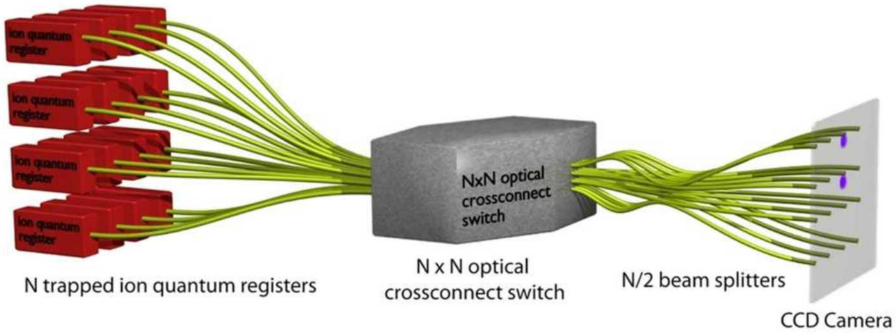

The Ytterbium Qubit

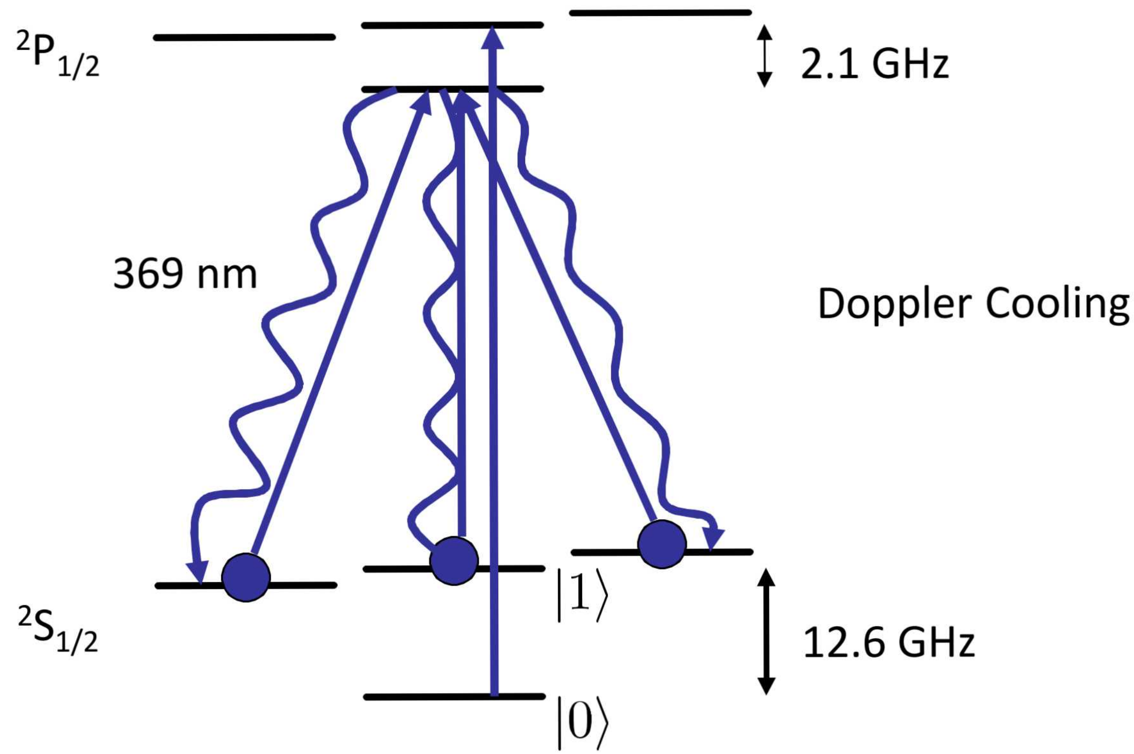

clock state qubit, magnetic field insensitive.

S. Olmschenk *et al.*, PRA **76**, 052314 (2007)

state initialization

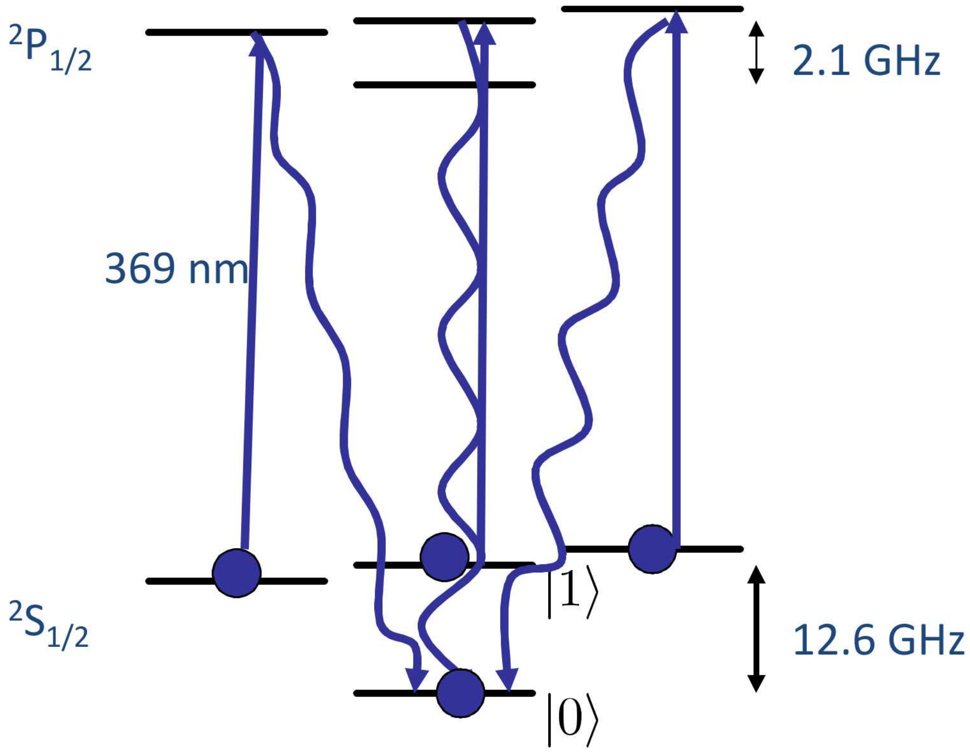

clock state qubit, magnetic field insensitive.

S. Olmschenk *et al.*, PRA **76**, 052314 (2007)

$^{171}Yb^{+}$ state detection

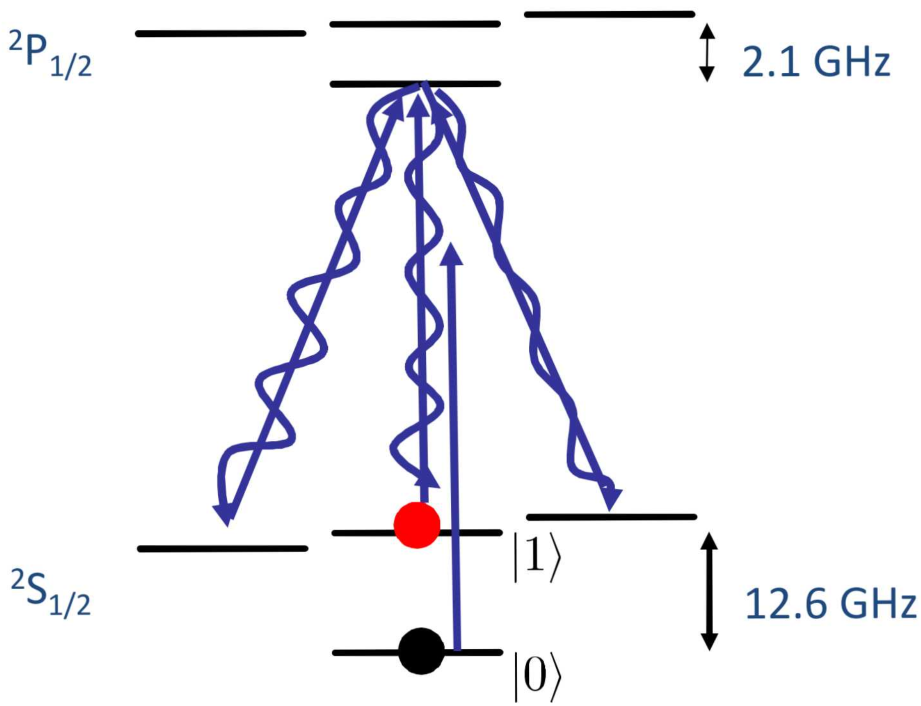

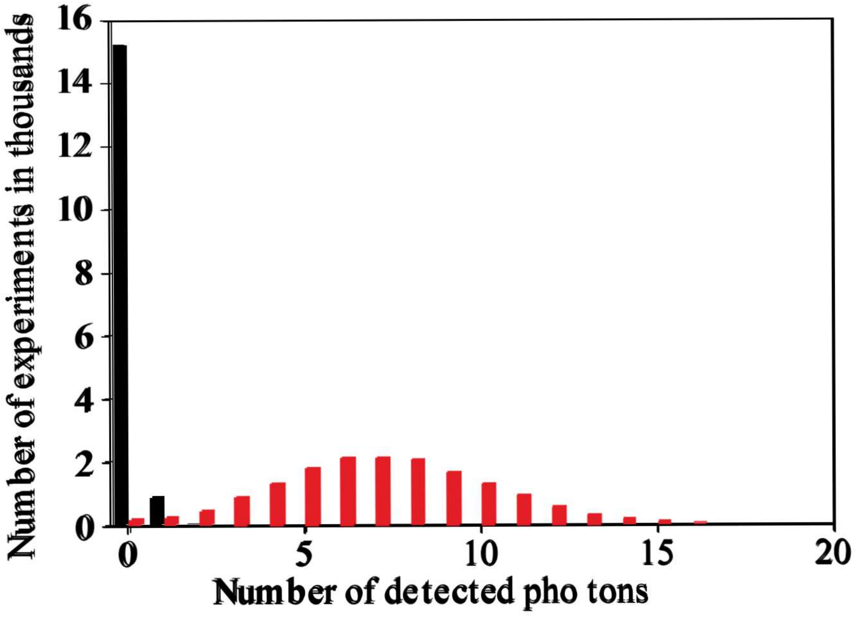

S. Olmschenk *et al.*, PRA **76**, 052314 (2007)

Swapping fidelity

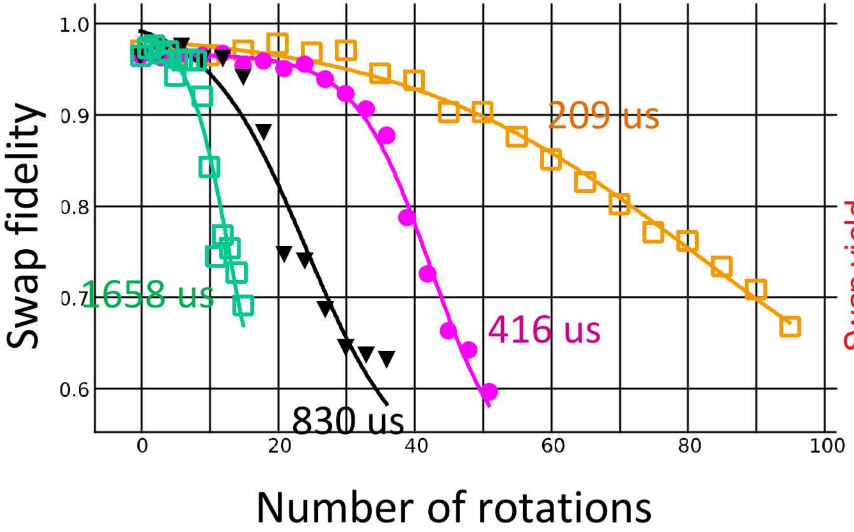

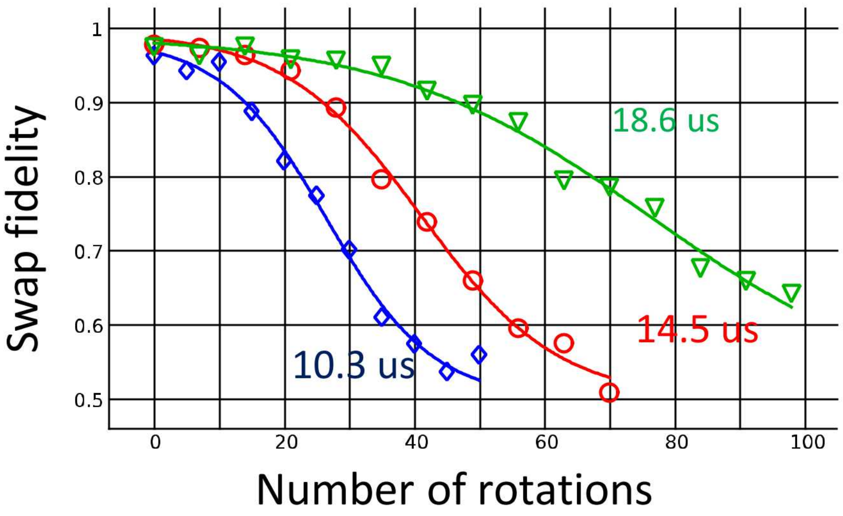

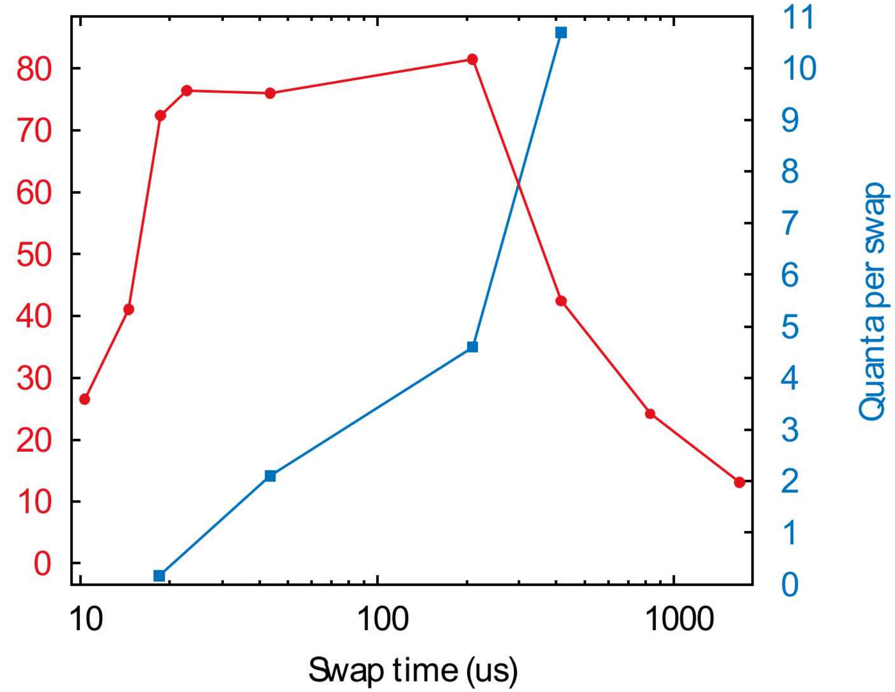

- Best fidelity between 20μs and 200μs
- Failure probability increases with number of swaps (heating)

HOA-2 heating rates

Heating rates as function of principal axes rotation

- Principal axes rotation measured by measuring π-times of Rabi flopping on cooled motional modes
- Minimal heating rates for motional mode parallel to trap surface $\dot{n}_{||}$
- Without technical noise: Vertical mode has at most $\dot{n}_{\perp} \leq 2\dot{n}_{||}$

  (P. Schindler, et al., Phys. Rev. A **92**, 013414 (2015).
- Limited by technical noise

$^{171}Yb^{+}$, Trap frequency 2.8 MHz, r.f. 50 MHz

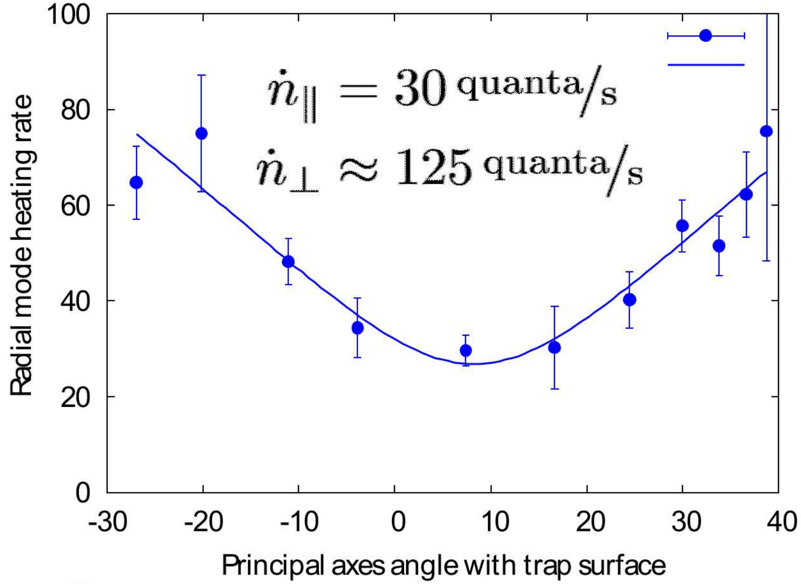

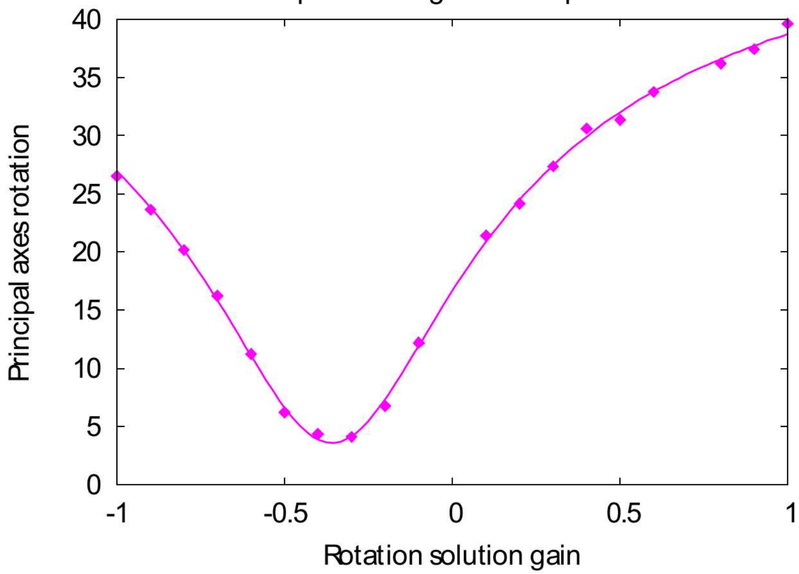

Compression of ion chains

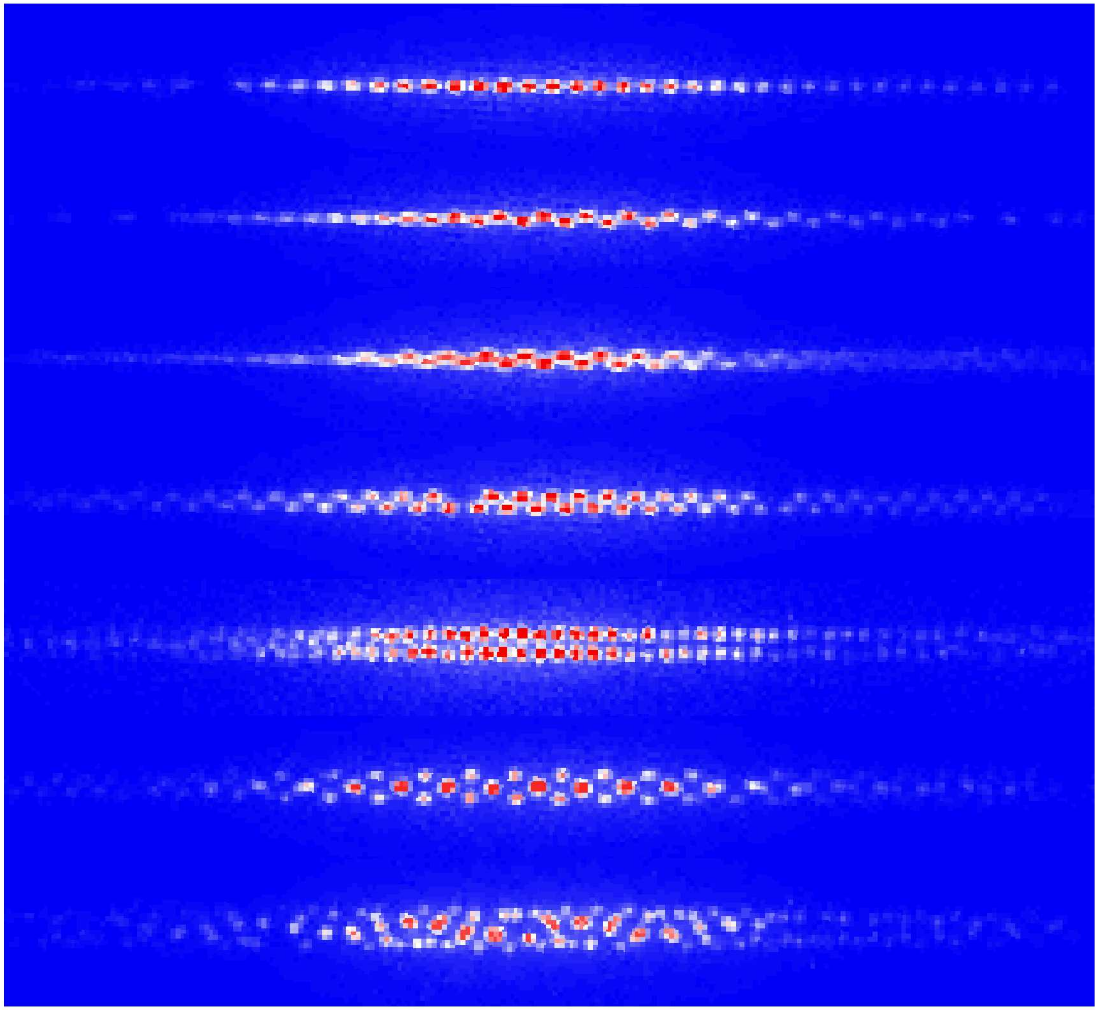

lifetime

15 min

1.5 hours

> 16 hours

Linear chain melting

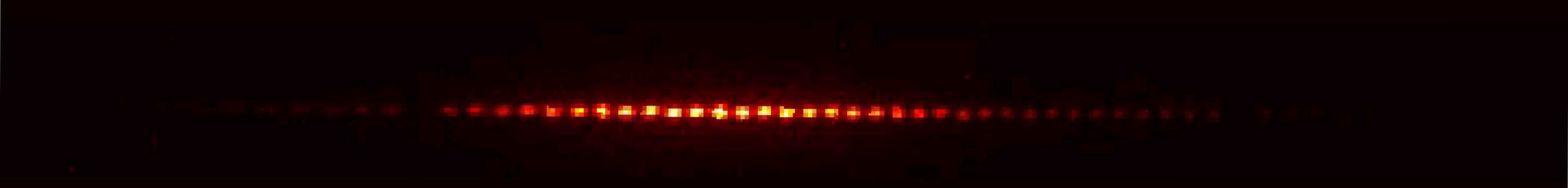

Slightly buckled chain stability

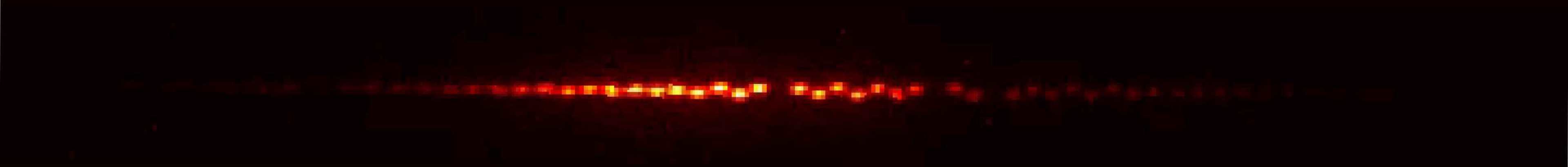

Ramping up buckling

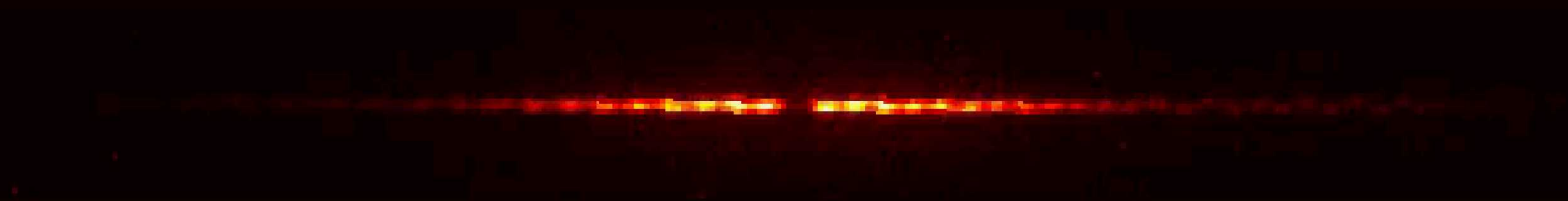

Ion “braid” stability